Available online at www.sciencedirect.com
ScienceDirect
Journal of Sound and Vibration 310 (2008) 287–312
JOURNAL OF SOUND AND VIBRATION
www.elsevier.com/locate/jsvi

# Continuous-time covariance approaches for modal analysis

Giuseppe Quaranta*, Pierangelo Masarati, Paolo Mantegazza

*Dipartimento di Ingegneria Aerospaziale, Politecnico di Milano via La Masa, 34 20156 Milano, Italy*

Received 25 July 2006; received in revised form 11 May 2007; accepted 30 July 2007
Available online 24 October 2007

**Abstract**

Proper orthogonal decomposition (POD) can be used to obtain complete information about the linear normal modes of structural systems only when special conditions are met, principally related to the knowledge of mass distribution and to the absence of damping. The main advantage of POD is the possibility to directly use covariance matrices estimated from time responses for the modal identification of the structure under investigation. This paper proposes a method to extend this covariance-based identification to general cases where significant damping is present and when no data is available on mass distribution. A least-square based decomposition is used to infer information about modal characteristics of the system. This decomposition is applied to three different cases: the first one uses records related to the free response of the system, while the remaining two use records of the system under persistent white noise excitations. In those latter cases the information on the excitation input time history can either be used, or treated as unknown. Basic, yet complete examples are presented to illustrate the properties of the proposed technique.


## 1. Introduction

The proper orthogonal decomposition (POD) is a powerful method, based on singular value decomposition (SVD), that is widely adopted to capture the dominant signals from the analysis of multidimensional time series. It has been applied, often with different denominations such as Karhunen–Loève Decomposition, in many branches of engineering, either for linear or nonlinear systems. For a good survey of the related literature, and for details on implementations and applications, the reader should refer to the work of Kershen et al. [1]. This technique has a much longer tradition in statistics, where is known as principal component analysis (PCA), aimed at the reduction of dimensionality in multivariate data set with the determination of a new set of variables which retains most of the *variation* present in the original set [2]. The first descriptions of the PCA can be traced back to the work of Pearson [3] in 1901 and Hotelling [4] in 1933. It can be easily shown that the optimal set of dimension $n$ is composed by the first $n$ eigenvectors of the covariance matrix ordered in terms of the magnitude of the related eigenvalues, which correspond to the first $n$ singular vectors of the observation matrix composed by the $m$ column vectors of the $p$ measures.

*Corresponding author. Tel.: +39 0223998362.
*E-mail addresses:* giuseppe.quaranta@polimi.it (G. Quaranta), pierangelo.masarati@polimi.it (P. Masarati), paolo.mantegazza@polimi.it (P. Mantegazza).

0022-460X/$ - see front matter © 2007 Elsevier Ltd. All rights reserved.
doi:10.1016/j.jsv.2007.07.078

Usually, POD analysis is applied to matrices describing the covariance of variables measured at the same time [1]. Other authors (e.g. Ref. [5]), compute covariance matrices of unsteady phenomena in the space of the samples, called *ensemble*, instead of in time. In any case, the dynamic relationship between consecutive samples in time, that the variables under investigation possess, appears to be not sufficiently taken into account by the POD, as it should. The reason is that POD does not explicitly take into account the cross-covariance between a measure and its derivative, assuming that both are available, to account for the dependency on the time shift between the measured variables [6].

In the structural dynamics field, special efforts have been dedicated to finding a physical interpretation for the POD modes [7–9]. Significant research effort has been dedicated to finding a correlation between the POD and the linear normal modes, which represent a more "classical" set of basic forms used for the dimensional reduction of dynamic structural systems, with the aim of using the POD as a modal analysis tool [9]. For undamped systems, Feeny and Kappagantu [7] showed that proper orthogonal modes (POMs) converge to the normal modes in free vibration analysis. The same holds true when random, white noise excitation is used [8,9]. However, in Ref. [9] it is stated that nothing can be said on the value of the frequency related to each mode if the mass distribution of the system is not known. As a consequence, additional frequency domain analysis of the POMs time series is required for the extraction of the related information [10–12]. Feeny and Kappagantu [7] formulated a hypothesis on the possible use of the derivatives of the state measures to solve the problem when damped systems are under investigation, but they did not pursue this research line. In order to recover the information on the frequency, Chelidze and Zhou [13] introduced what they called smooth orthogonal decomposition (SOD), which uses a numerically approximated covariance matrix of the derivatives of the measures, together with the usual covariance of the measures, to obtain additional information. However, this method suffers from the limitation of being exactly applicable only to undamped systems, and only provides an estimate of the frequency as the sample time increases.

To overcome all these problems, and to derive a more general method to recover the information on the dynamic characteristics of the system under investigation using covariance matrices, another method is here introduced. This method originates from the simple observation that least squares can be used to extract the eigenvalues and eigenvectors of a mechanical system from its time response. The proposed methodology works for generally damped systems and allows the identification of modal forms with the related eigenvalues without any prior knowledge of the mass distribution. The possibility to identify damped systems is extremely important when structures, like aircraft, interacting with the surrounding fluid, are investigated. The crucial piece of information, neglected by other authors in previous works, is the cross-covariance matrix between the measures and their derivatives, as shown in Section 2. Of course, this means that the measure derivatives must be either acquired, or somehow restored from the known data using a finite difference numerical operator, as in Ref. [13]. In any case, since the numerical differentiation is known to introduce additional noise in the signals, an integral numerical operator can be used, which acts as a filter instead. In this case, the role of the basic signals is played by the integrated ones, while the measured signals act as their derivatives.

Section 2 presents the basic idea introducing a new orthogonal decomposition of the data which could be denominated *proper dynamic decomposition* (PDD), since it started as an extension of the POD methods taking into account the fact that the time series under analysis are observations of a dynamic system data. Section 3 gives an interpretation of the obtained modes when free responses are used as time histories, which directly allows to recover the normal modes of the system, together with the associated frequency and damping values. Section 4 gives an interpretation for the case of responses obtained from persistent excitations, which again allows to recover the normal modes, with the associated frequency and damping. The last two sections are completed by simple examples, both analytical and numerical, to illustrate the quality of the proposed method. Incidentally, what is presented results in a methodology to recover the information on the characteristics of the dynamics of the system under analysis directly by a continuous time domain approach instead of going through a preliminary discrete identification, even though this was not an objective of the work.

## 2. Transient response analysis

Consider a set of measures $\mathbf{x}(t) \in \mathbb{R}^m$, that are functions of time $t \in [0, \tau]$, obtained as free responses of a linear system subjected to a perturbation of its initial conditions. This set may be combined with a constant,

unknown vector $\mathbf{\Phi} \in \mathbb{C}^m$

$$q = \mathbf{x}^{\mathrm{T}}\mathbf{\Phi} \tag{1}$$

to yield a scalar function $q(t) \in \mathbb{C}^1$ that satisfies the linear differential equation

$$\dot{q} = \lambda q, \tag{2}$$

where $\lambda \in \mathbb{C}$ is unknown.[1]

The aim of the proposed analysis is to represent the generic transient response, not limited to the free response of a dynamic system, into a set of generic modes, and thus can be viewed as a PDD. The resulting PDD, consisting in the proper dynamic modes (PDMs) $\mathbf{\Phi}$ and the corresponding proper dynamic values (PDVs) $\lambda$, represents a decomposition of the analyzed signals in a minimal set of damped harmonic signals of the type $\mathbf{\Phi}_i e^{\lambda_i t}$, which can be combined with the conjugate solution, when complex, to obtain the real expression

$$\mathbf{x}(t) = e^{\mathrm{Re}(\lambda_i)t}(\mathrm{Re}(\mathbf{\Phi}_i)\cos(\mathrm{Im}(\lambda_i)t) + \mathrm{Im}(\mathbf{\Phi}_i)\sin(\mathrm{Im}(\lambda_i)t)). \tag{3}$$

The classification of the PDMs can be done in terms of frequency, damping or both, depending on the specific properties sought for the PDD. It is worth stressing that only the eigensolutions observable with the considered measures can be effectively recovered using this type of analysis.

In general, Eq. (2) cannot be strictly satisfied by a generic vector $\mathbf{\Phi}$, so the problem

$$\dot{\mathbf{x}}^{\mathrm{T}}\mathbf{\Phi} \cong \lambda \mathbf{x}^{\mathrm{T}}\mathbf{\Phi} \tag{4}$$

yields a residual error $\varepsilon$:

$$(\lambda\mathbf{x} - \dot{\mathbf{x}})^{\mathrm{T}}\mathbf{\Phi} = \varepsilon, \tag{5}$$

which needs to be minimized to obtain an optimal vector $\mathbf{\Phi}$. An integral measure of the overall square error over the measure interval $[0, \tau]$ is

$$J = \frac{1}{2\tau}\int_0^\tau \varepsilon^2 \,\mathrm{d}t, \tag{6}$$

which can be minimized by an appropriate selection of the multipliers $\mathbf{\Phi}$:

$$\min_{\mathbf{\Phi}}(J). \tag{7}$$

The minimization with respect to $\mathbf{\Phi}$ of Eq. (6) leads to

$$\begin{aligned}\frac{\partial J}{\partial \mathbf{\Phi}} &= \frac{1}{\tau}\left(\int_0^\tau (\lambda\mathbf{x} - \dot{\mathbf{x}})(\lambda\mathbf{x} - \dot{\mathbf{x}})^{\mathrm{T}}\,\mathrm{d}t\right)\mathbf{\Phi} \\ &= \left(\lambda^2\frac{1}{\tau}\int_0^\tau \mathbf{x}\mathbf{x}^{\mathrm{T}}\,\mathrm{d}t - \lambda\frac{1}{\tau}\int_0^\tau (\dot{\mathbf{x}}\mathbf{x}^{\mathrm{T}} + \mathbf{x}\dot{\mathbf{x}}^{\mathrm{T}})\,\mathrm{d}t + \frac{1}{\tau}\int_0^\tau \dot{\mathbf{x}}\dot{\mathbf{x}}^{\mathrm{T}}\,\mathrm{d}t\right)\mathbf{\Phi} \\ &= (\lambda^2\mathbf{\Sigma}_{\mathbf{xx}} - \lambda(\mathbf{\Sigma}_{\dot{\mathbf{x}}\mathbf{x}} + \mathbf{\Sigma}_{\mathbf{x}\dot{\mathbf{x}}}) + \mathbf{\Sigma}_{\dot{\mathbf{x}}\dot{\mathbf{x}}})\mathbf{\Phi} = \mathbf{0},\end{aligned} \tag{8}$$

which represents a second-order eigenproblem, where $\lambda$ is the eigenvalue and $\mathbf{\Phi}$ is the eigenvector [14]. If either the mean value of the vector $\mathbf{x}$ is null, or it is removed, the matrices $\mathbf{\Sigma}_{\mathbf{xx}}$ and $\mathbf{\Sigma}_{\dot{\mathbf{x}}\dot{\mathbf{x}}} \in \mathbb{R}^{m\times m}$ represent the *deterministic auto-covariances* (often simply denominated *covariances*) of the state and of its time derivative, respectively (for a definition of covariances see, Ref. [15]). The adjective "deterministic" is added to emphasize the fact that these matrices only converge toward the "statistical" variances for $\tau \to \infty$. In this sense, as opposed to the usual meaning of "non-randomly forced", it was already used in Ref. [16]. However, that qualification will be dropped in the following to simplify the language, since the meaning should be clear from the context.

These covariance matrices are usually the piece of information used for the extraction of POD which is composed by the proper orthogonal values (POVs), the eigenvalues of $\mathbf{\Sigma}_{\mathbf{xx}}$, and the corresponding modes

[1]Actually, since $\mathbf{x} \in \mathbb{R}^m$, for each $\lambda \in \mathbb{C}$ with $\mathrm{Im}(\lambda) \neq 0$ there will exist conjugates $\lambda^*$, $\mathbf{\Phi}^*$ such that $q + q^*, \dot{q} + \dot{q}^* \in \mathbb{R}^1$, and $j(q - q^*)$, $j(\dot{q} - \dot{q}^*) \in \mathbb{R}^1$.

(POMs) [1]. The matrix $\mathbf{\Sigma}_{\dot{\mathbf{x}}\mathbf{x}}$ represents the *cross-covariance* between the state derivative and the state itself, while, by definition, it may be shown that $\mathbf{\Sigma}_{\mathbf{x}\dot{\mathbf{x}}} = \mathbf{\Sigma}_{\dot{\mathbf{x}}\mathbf{x}}^{\mathrm{T}}$. The latter matrix plays a crucial role for the correct identification of eigensolutions when significant damping is present, as shown in the following.

The resulting eigenproblem is not in general related to the system state matrix, but represents a least square approximation of the generic transient response problem into a set of complex modes (PDMs). In a fashion similar to the SOD decomposition presented in Ref. [13], this PDD is invariant with respect to any linear, non-singular coordinate transformation. In fact, if a new set of coordinates $\mathbf{y} = \mathbf{T}\mathbf{x}$ is defined, Eq. (8) becomes

$$\left(\tilde{\lambda}^2 \frac{1}{\tau}\int_0^\tau \mathbf{T}\mathbf{x}\mathbf{x}^{\mathrm{T}}\mathbf{T}^{\mathrm{T}}\,\mathrm{d}t - \tilde{\lambda}\frac{1}{\tau}\int_0^\tau (\mathbf{T}\dot{\mathbf{x}}\mathbf{x}^{\mathrm{T}}\mathbf{T}^{\mathrm{T}} + \mathbf{T}\mathbf{x}\dot{\mathbf{x}}^{\mathrm{T}}\mathbf{T}^{\mathrm{T}})\,\mathrm{d}t + \frac{1}{\tau}\int_0^\tau \mathbf{T}\dot{\mathbf{x}}\dot{\mathbf{x}}^{\mathrm{T}}\mathbf{T}^{\mathrm{T}}\,\mathrm{d}t\right)\tilde{\mathbf{\Phi}}$$
$$= (\tilde{\lambda}^2\mathbf{T}\mathbf{\Sigma}_{\mathbf{x}\mathbf{x}}\mathbf{T}^{\mathrm{T}} - \tilde{\lambda}\mathbf{T}(\mathbf{\Sigma}_{\dot{\mathbf{x}}\mathbf{x}} + \mathbf{\Sigma}_{\mathbf{x}\dot{\mathbf{x}}})\mathbf{T}^{\mathrm{T}} + \mathbf{T}\mathbf{\Sigma}_{\dot{\mathbf{x}}\dot{\mathbf{x}}}\mathbf{T}^{\mathrm{T}})\tilde{\mathbf{\Phi}} = \mathbf{0}.$$

Considering that $\tilde{\mathbf{\Phi}} = \mathbf{T}^{-\mathrm{T}}\mathbf{\Phi}$, the left-multiplication of the last equation by $\mathbf{T}^{-1}$ easily shows that $\tilde{\lambda} = \lambda$.

### 2.1. Requirements on measure availability

The proposed approach requires a set of measures $\mathbf{x}$ and its time-derivatives $\dot{\mathbf{x}}$. In practical applications (system identification from numerical simulation output, or from experimental measurements), different combinations of measures may be available. Typically, in case of numerical simulations, the entire state and its derivatives is available; however, when only partial information is available, the missing part needs to be estimated.

When only position measures $\mathbf{y}$ are available, velocities $\dot{\mathbf{y}}$ and accelerations $\ddot{\mathbf{y}}$ can be computed by numerical differentiation. This is likely to yield significantly noisy derivatives, unless appropriate filtering is used. In this work, centered differences,

$$\dot{\mathbf{y}}_k = \frac{\mathbf{y}_{k+1} - \mathbf{y}_{k-1}}{2\Delta t} \tag{9}$$

$$\ddot{\mathbf{y}}_k = \frac{\dot{\mathbf{y}}_{k+1} - \dot{\mathbf{y}}_{k-1}}{2\Delta t}, \tag{10}$$

have been used to compute position derivatives. Centered differences have been selected to avoid phase shift in the derivatives.

When only acceleration measures $\ddot{\mathbf{y}}$ are available, velocities $\dot{\mathbf{y}}$ and positions $\mathbf{y}$ can be computed by numerical integration. This process is expected to naturally filter out measurement noise. In this work, this second approach has not been directly used; however, non-trivial numerical problems have been usually integrated using Matlab standard integration algorithms, basically resulting in a form of numerical integration of the accelerations. Future work will address the practical application of this technique to experimental measures.

## 3. Free response

Consider Eq. (4) before multiplication by vector $\mathbf{\Phi}$,

$$\dot{\mathbf{x}} \cong \lambda\mathbf{x}, \tag{11}$$

where the actual system can be represented by a simple, constant coefficient autoregressive (AR) model

$$\dot{\mathbf{x}} = \mathbf{A}\mathbf{x}, \tag{12}$$

with $\mathbf{A} \in \mathbb{R}^{m\times m}$. In this case, Eq. (5) can be written as

$$(\lambda\mathbf{x} - \mathbf{A}\mathbf{x})^{\mathrm{T}}\mathbf{\Phi} = \varepsilon. \tag{13}$$

The same minimization procedure as in Eq. (8) leads to

$$\frac{\partial J}{\partial \mathbf{\Phi}} = \left(\frac{1}{\tau}\int_0^\tau (\lambda\mathbf{I} - \mathbf{A})\mathbf{x}\mathbf{x}^{\mathrm{T}}(\lambda\mathbf{I} - \mathbf{A}^{\mathrm{T}})\,\mathrm{d}t\right)\mathbf{\Phi}$$
$$= (\lambda\mathbf{I} - \mathbf{A})\frac{1}{\tau}\int_0^\tau \mathbf{x}\mathbf{x}^{\mathrm{T}}\,\mathrm{d}t(\lambda\mathbf{I} - \mathbf{A}^{\mathrm{T}})\mathbf{\Phi}$$

$$= ((\lambda \mathbf{I} - \mathbf{A})\boldsymbol{\Sigma}_{\mathbf{xx}}(\lambda \mathbf{I} - \mathbf{A}^{\mathrm{T}}))\boldsymbol{\Phi} \tag{14}$$

$$= (\lambda^2 \boldsymbol{\Sigma}_{\mathbf{xx}} - \lambda(\mathbf{A}\boldsymbol{\Sigma}_{\mathbf{xx}} + \boldsymbol{\Sigma}_{\mathbf{xx}}\mathbf{A}^{\mathrm{T}}) + \mathbf{A}\boldsymbol{\Sigma}_{\mathbf{xx}}\mathbf{A}^{\mathrm{T}})\boldsymbol{\Phi}. \tag{15}$$

Considering Eq. (8), the following correspondences can be recognized:

$$\boldsymbol{\Sigma}_{\dot{\mathbf{x}}\mathbf{x}} = \mathbf{A}\boldsymbol{\Sigma}_{\mathbf{xx}} \tag{16}$$

$$\begin{aligned} \boldsymbol{\Sigma}_{\dot{\mathbf{x}}\dot{\mathbf{x}}} &= \mathbf{A}\boldsymbol{\Sigma}_{\mathbf{xx}}\mathbf{A}^{\mathrm{T}} \\ &= \boldsymbol{\Sigma}_{\dot{\mathbf{x}}\mathbf{x}}\mathbf{A}^{\mathrm{T}} \\ &= \mathbf{A}\boldsymbol{\Sigma}_{\mathbf{x}\dot{\mathbf{x}}}. \end{aligned} \tag{17}$$

The essential difference is that the covariance matrices of Eq. (15) result from the free response of a linear system, so they exactly contain the dynamics of matrix $\mathbf{A}$, while those of Eq. (8) describe a generic transient response.

Two different estimates of matrix $\mathbf{A}$ can be obtained from the covariances of a free response analysis,

$$\overline{\mathbf{A}} = \boldsymbol{\Sigma}_{\dot{\mathbf{x}}\mathbf{x}}\boldsymbol{\Sigma}_{\mathbf{xx}}^{-1}, \tag{18}$$

$$\overline{\overline{\mathbf{A}}} = \boldsymbol{\Sigma}_{\dot{\mathbf{x}}\dot{\mathbf{x}}}\boldsymbol{\Sigma}_{\mathbf{x}\dot{\mathbf{x}}}^{-1}, \tag{19}$$

where Eq. (18) corresponds to the classical AR identification resulting from the application of least-squares [17].

Expression (14) highlights the fact that the previously mentioned second-order eigenproblem, in this specific case, is actually the product of problem (13) and its transpose. But, since the eigenvalues of $\mathbf{A}$ and of $\mathbf{A}^{\mathrm{T}}$ are the same [18], the eigenvalues of the second-order problem are twice those of matrix $\mathbf{A}$. They can be obtained, for example, from either of the problems

$$(\boldsymbol{\Sigma}_{\mathbf{x}\dot{\mathbf{x}}} - \lambda\boldsymbol{\Sigma}_{\mathbf{xx}})\mathbf{x} = \mathbf{0}, \tag{20}$$

$$(\boldsymbol{\Sigma}_{\dot{\mathbf{x}}\dot{\mathbf{x}}} - \lambda\boldsymbol{\Sigma}_{\dot{\mathbf{x}}\mathbf{x}})\mathbf{x} = \mathbf{0}. \tag{21}$$

In case of exact covariance matrices from measurements of the free response of a linear, time invariant system, the use of either of Eqs. (20), (21) is perfectly equivalent, while Eq. (8) leads to a problem of twice the size, whose eigenvalues are the combination of those of Eqs. (20), (21), which means that each eigenvalue is present twice. If data is either obtained numerically or experimentally, or if portions of data need to be reconstructed by either numerical integration or differentiation, as discussed in Section 2.1, the formula among those of Eqs. (20), (21) that uses the covariance matrices less affected by errors should be chosen. Further details and examples are presented in subsequent sections, when discussing numerical results.

In case of a system response which is *stationary* in a statistical sense,[2] which means that the covariance matrices only depend on the time shift between the process vectors, so the covariances at zero time shift do not depend on the sampling instant of time [15]. In this case it is well known that each scalar process is orthogonal to its first derivative [15], so the cross-covariance between each state and its derivative will tend to a null value when the time is increased in order to make the time process statistically relevant. More generally, for a vector state $\mathbf{x}$ one can show that

$$E\left[\dot{\mathbf{x}}\mathbf{x}^{\mathrm{T}}\right] + E\left[\mathbf{x}\dot{\mathbf{x}}^{\mathrm{T}}\right] = E\left[\frac{\mathrm{d}}{\mathrm{d}t}(\mathbf{x}\mathbf{x}^{\mathrm{T}})\right]. \tag{22}$$

The expectation operator $E[\cdot]$ for an ergodic process applied to the right-hand side of Eq. (22) is equivalent to

$$\lim_{\tau\to\infty}\frac{1}{2\tau}\int_{-\tau}^{\tau}\frac{\mathrm{d}}{\mathrm{d}t}(\mathbf{x}\mathbf{x}^{\mathrm{T}}) = \lim_{\tau\to\infty}\frac{\mathbf{x}(\tau)\mathbf{x}^{\mathrm{T}}(\tau) - \mathbf{x}(-\tau)\mathbf{x}^{\mathrm{T}}(-\tau)}{2\tau} = \mathbf{0}. \tag{23}$$

[2]Actually, for the presented cases, the process must be *ergodic* since the means are taken as time averages and not as ensemble averages [6].

So, after a sufficient amount of time, the expectations included in Eq. (22) will become equal to the corresponding cross-covariance matrices, or, in other words, the deterministic covariances will match the statistical ones. As a consequence, it is possible to affirm that for a stationary process

$$\lim_{\tau\to\infty}(\mathbf{\Sigma}_{\dot{\mathbf{x}}\mathbf{x}}+\mathbf{\Sigma}_{\mathbf{x}\dot{\mathbf{x}}})=\mathbf{0}, \tag{24}$$

which means that the cross-covariance between the state and its derivative is a skew-symmetric matrix. Exploiting Eq. (24) in Eq. (8) highlights that for stationary systems

$$(\lambda^2\mathbf{\Sigma}_{\mathbf{xx}}+\mathbf{\Sigma}_{\dot{\mathbf{x}}\dot{\mathbf{x}}})\mathbf{\Phi}=\mathbf{0}. \tag{25}$$

A typical case where the transient process is stationary is that related to structural systems with no damping. In this case, after an initial state perturbation, the system starts oscillating with constant amplitude and Eq. (24) remains valid for all times in the statistical sense. As a consequence, the eigensolution can be computed without using the information included in the cross-covariance matrix, as indicated by Chelidze and Zhou [13].

The transient analysis is now applied to selected analytical and numerical cases to highlight its versatility and soundness.

### 3.1. Single degree of freedom undamped oscillator

Consider the simplest example: the free response of an undamped mass-spring system for a given initial displacement. The correct model requires to include the entire state vector, which is composed by the position and velocity of the oscillator, so

$$\mathbf{x}=y_0\begin{Bmatrix}\cos(\omega_0 t)\\ -\omega_0\sin(\omega_0 t)\end{Bmatrix}, \tag{26}$$

where $\omega_0=\sqrt{k/m}$; its derivative is

$$\dot{\mathbf{x}}=-\omega_0 y_0\begin{Bmatrix}\sin(\omega_0 t)\\ \omega_0\cos(\omega_0 t)\end{Bmatrix}. \tag{27}$$

To obtain the covariance and cross-covariance matrices, the contributions to integrand expression included in Eq. (8),

$$\mathbf{x}\mathbf{x}^{\mathrm{T}}=y_0^2\begin{bmatrix}\cos^2(\omega_0 t) & -\omega_0\cos(\omega_0 t)\sin(\omega_0 t)\\ -\omega_0\cos(\omega_0 t)\sin(\omega_0 t) & \omega_0^2\sin^2(\omega_0 t)\end{bmatrix}, \tag{28}$$

$$\mathbf{x}\dot{\mathbf{x}}^{\mathrm{T}}=y_0^2\begin{bmatrix}-\omega_0\cos(\omega_0 t)\sin(\omega_0 t) & -\omega_0^2\cos^2(\omega_0 t)\\ \omega_0^2\sin^2(\omega_0 t) & \omega_0^3\cos(\omega_0 t)\sin(\omega_0 t)\end{bmatrix}, \tag{29}$$

$$\dot{\mathbf{x}}\dot{\mathbf{x}}^{\mathrm{T}}=y_0^2\begin{bmatrix}\omega_0^2\sin^2(\omega_0 t) & \omega_0^3\cos(\omega_0 t)\sin(\omega_0 t)\\ \omega_0^3\cos(\omega_0 t)\sin(\omega_0 t) & \omega_0^4\cos^2(\omega_0 t)\end{bmatrix} \tag{30}$$

are computed. If $\tau$ is a multiple of half of the oscillation period, namely $\tau=N\pi/\omega_0$ with $N\in\mathbb{N}$, the integrals of the mixed sine–cosine terms vanish; at the same time, the integrals of the squared sines and cosines are equal to $N\pi/2\omega_0$, so:

$$\mathbf{\Sigma}_{\mathbf{xx}}=\frac{\omega_0}{N\pi}\int_0^{N\pi/\omega_0}\mathbf{x}\mathbf{x}^{\mathrm{T}}\,\mathrm{d}t=\frac{1}{2}y_0^2\begin{bmatrix}1 & 0\\ 0 & \omega_0^2\end{bmatrix}, \tag{31}$$

$$\mathbf{\Sigma}_{\mathbf{x}\dot{\mathbf{x}}}=\frac{\omega_0}{N\pi}\int_0^{N\pi/\omega_0}\mathbf{x}\dot{\mathbf{x}}^{\mathrm{T}}\,\mathrm{d}t=\frac{1}{2}y_0^2\begin{bmatrix}0 & -\omega_0^2\\ \omega_0^2 & 0\end{bmatrix}, \tag{32}$$

$$\mathbf{\Sigma}_{\dot{\mathbf{x}}\dot{\mathbf{x}}} = \frac{\omega_0}{N\pi}\int_0^{N\pi/\omega_0} \dot{\mathbf{x}}\dot{\mathbf{x}}^{\mathrm{T}}\,\mathrm{d}t = \frac{1}{2}y_0^2\begin{bmatrix}\omega_0^2 & 0\\ 0 & \omega_0^4\end{bmatrix}. \tag{33}$$

The cross-covariance matrix in Eq. (32) is skew symmetric as expected. The eigenproblem of Eq. (8), after some trivial simplifications, becomes

$$\left(\lambda^2\begin{bmatrix}1 & 0\\ 0 & \omega_0^2\end{bmatrix} + \begin{bmatrix}\omega_0^2 & 0\\ 0 & \omega_0^4\end{bmatrix}\right)\mathbf{\Phi} = \mathbf{0}. \tag{34}$$

Its characteristic equation

$$\omega_0^2(\lambda^2 + \omega_0^2)^2 = 0. \tag{35}$$

consists in two independent, and identical, sub-eigenproblems. In this case the complete state seems to be unnecessary, since the equation that relates the covariance of the position with the covariance of the velocity is enough to obtain a problem with the same eigenvalue (which appears once only instead of twice, by the way). However, this is true for this special case only, as shown in the following. Furthermore, using the formulas presented in Eqs. (18), (19) the complete expression of the state matrix can be recovered.

In a general case, where the covariances are computed over an arbitrary interval $[0, \tau]$, after defining

$$\alpha_s = \frac{\sin(2\omega_0\tau)}{2\omega_0\tau}, \tag{36}$$

$$\alpha_c = \frac{1-\cos(2\omega_0\tau)}{2\omega_0\tau}, \tag{37}$$

which both vanish whenever $\tau = N\pi/\omega_0$ ($\alpha_s$ also vanishes for $\tau = N\pi/(2\omega_0)$), the covariance matrices result in

$$\mathbf{\Sigma}_{\mathbf{xx}} = \frac{1}{\tau}\int_0^{\tau} \mathbf{x}\mathbf{x}^{\mathrm{T}}\mathrm{d}t = y_0^2\begin{bmatrix}(1+\alpha_s) & -\omega_0\alpha_c\\ -\omega_0\alpha_c & \omega_0^2(1-\alpha_s)\end{bmatrix} \tag{38}$$

$$\mathbf{\Sigma}_{\mathbf{x}\dot{\mathbf{x}}} = \frac{1}{\tau}\int_0^{\tau} \mathbf{x}\dot{\mathbf{x}}^{\mathrm{T}}\mathrm{d}t = y_0^2\begin{bmatrix}-\omega_0\alpha_c & -\omega_0^2(1+\alpha_s)\\ \omega_0^2(1-\alpha_s) & \omega_0^3\alpha_c\end{bmatrix} \tag{39}$$

$$\mathbf{\Sigma}_{\dot{\mathbf{x}}\dot{\mathbf{x}}} = \frac{1}{\tau}\int_0^{\tau} \dot{\mathbf{x}}\dot{\mathbf{x}}^{\mathrm{T}}\mathrm{d}t = y_0^2\begin{bmatrix}\omega_0^2(1-\alpha_s) & \omega_0^3\alpha_c\\ \omega_0^3\alpha_c & \omega_0^4(1+\alpha_s)\end{bmatrix} \tag{40}$$

The cross-covariance is no longer structurally skew-symmetric, since the process can be considered perfectly stationary only if a multiple of the fundamental period is considered as $\tau$. The eigenproblem of Eq. (8) becomes

$$\left(\lambda^2\begin{bmatrix}(1+\alpha_s) & -\omega_0\alpha_c\\ -\omega_0\alpha_c & \omega_0^2(1-\alpha_s)\end{bmatrix} + 2\lambda\begin{bmatrix}-\omega_0\alpha_c & -\omega_0^2\alpha_s\\ -\omega_0^2\alpha_s & \omega_0^3\alpha_c\end{bmatrix} + \begin{bmatrix}\omega_0^2(1-\alpha_s) & \omega_0^3\alpha_c\\ \omega_0^3\alpha_c & \omega_0^4(1+\alpha_s)\end{bmatrix}\right)\mathbf{\Phi} = \mathbf{0}, \tag{41}$$

which again, after some manipulation, yields the characteristic equation

$$\omega_0^2(\lambda^2 + \omega_0^2)^2(1 - \alpha_s^2 - \alpha_c^2) = 0, \tag{42}$$

which gives the same roots of the two sub-eigenproblems of Eq. (35), regardless of the value of $\tau$.

Excluding the cross-covariance, or considering only a partial state, without the velocity $\dot{y}$, leads to an incorrect result. While the latter case does not lead to any useful information, the former one is easily proved by considering that, by neglecting the cross-covariance term, Eq. (41) becomes

$$\left(\lambda^2\begin{bmatrix}(1+\alpha_s) & -\omega_0\alpha_c\\ -\omega_0\alpha_c & \omega_0^2(1-\alpha_s)\end{bmatrix} + \begin{bmatrix}\omega_0^2(1-\alpha_s) & \omega_0^3\alpha_c\\ \omega_0^3\alpha_c & \omega_0^4(1+\alpha_s)\end{bmatrix}\right)\mathbf{\Phi} = \mathbf{0}, \tag{43}$$

resulting in the characteristic equation

$$\lambda^4 + 2\omega_0^2\lambda^2 \frac{1 + \frac{2}{(2\omega_0\tau)^2}(1 - \cos(2\omega_0\tau))}{1 - \frac{2}{(2\omega_0\tau)^2}(1 - \cos(2\omega_0\tau))} + \omega_0^4 = 0, \tag{44}$$

whose solution eventually converges, oscillating, to the expected value

$$\lim_{\tau\to\infty} \lambda^2 = -\omega_0^2, \tag{45}$$

with multiplicity 2. The exact solution is also obtained when $\tau$ is an integer multiple of $\pi/\omega_0$.

### 3.2. Single degree of freedom damped oscillator

Consider now the free response of a damped mass-spring system for a given initial displacement

$$\mathbf{x} = y_0 e^{-\xi\omega_0 t} \begin{Bmatrix} \cos(\sqrt{1-\xi^2}\omega_0 t) \\ -\omega_0 \sin(\sqrt{1-\xi^2}\omega_0 t + \phi) \end{Bmatrix}, \tag{46}$$

where $\xi = r/\sqrt{4km}$ and $\phi = \sin^{-1}(\xi)$; its derivative is

$$\dot{\mathbf{x}} = -\omega_0 y_0 e^{-\xi\omega_0 t} \begin{Bmatrix} \sin(\sqrt{1-\xi^2}\omega_0 t + \phi) \\ \omega_0 \cos(\sqrt{1-\xi^2}\omega_0 t + 2\phi) \end{Bmatrix}. \tag{47}$$

In this case, the cross-covariance $\mathbf{\Sigma}_{\dot{\mathbf{x}}\mathbf{x}}$ is no longer skew-symmetric during the transient at any time. However, it must be noticed that all covariance matrices tend to a null value while $\tau \to \infty$ since the system is asymptotically stable, so the proposed analysis is valid while the transient is developing and not when the steady-state condition is reached.

A numerical solution of the problem, with $\omega_0 = 2\pi$ and a significant damping $\xi = 0.2$, clearly illustrates the beneficial effect of the cross-covariance $\mathbf{\Sigma}_{\dot{\mathbf{x}}\mathbf{x}}$ between the derivative of state and the state itself in the identification of the properties of the system. Fig. 1 illustrates the time history of the free response of the system for a perturbation of the initial value of the state; a 0.01 s time step is used. A logarithmic scale is used for the time axis to improve readability, since the highly damped response quickly vanishes. Fig. 2 shows the coefficients of the $\mathbf{\Sigma}_{\mathbf{xx}}$ (left) and $\mathbf{\Sigma}_{\dot{\mathbf{x}}\mathbf{x}}$ (right) covariance matrices. They clearly undergo large variations, but nonetheless the identification is very accurate right from the beginning, as shown in Fig. 3, which presents the errors in the real (left) and imaginary (right) parts of the eigenvalue. They are very limited (below 1e − 4) for every time since the first time step, as soon as one measure, plus the initial conditions, is available to

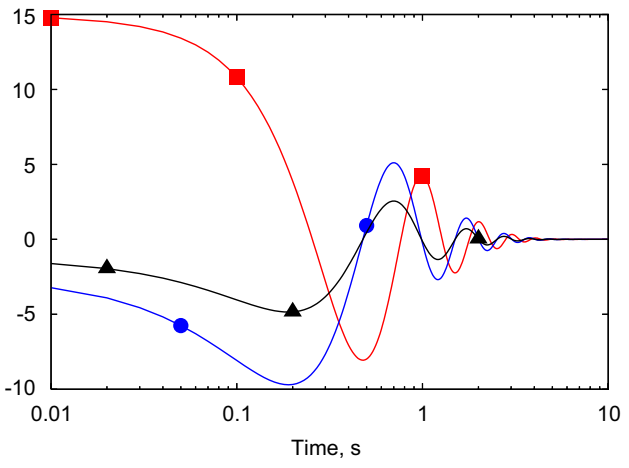


Fig. 1. Time history of the response of a damped, single degree of freedom, oscillating system: acceleration (▲); position (■) and velocity (●) signals are scaled for clarity (respectively ×15 and ×2).

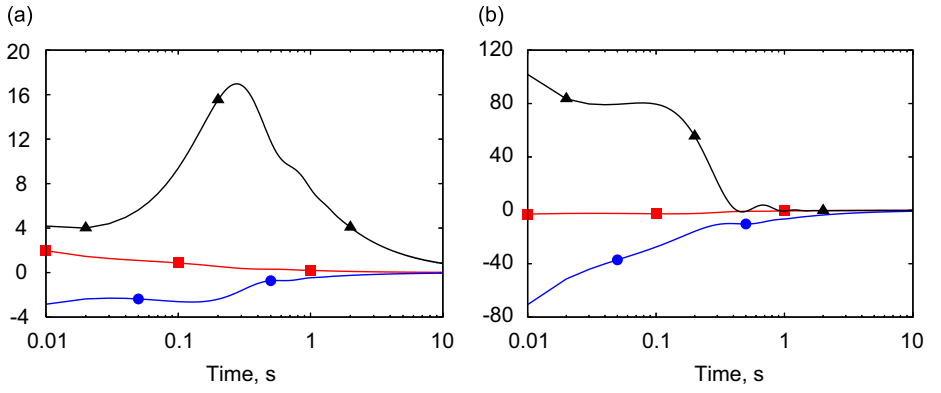


Fig. 2. Time history of the $\mathbf{\Sigma_{xx}}$ (a) and $\mathbf{\Sigma_{\dot{x}\dot{x}}}$ (b) covariance matrix coefficients of a damped, single degree of freedom, oscillating system: (1, 1) (■); (1, 2) (•); (2, 2) (▲).

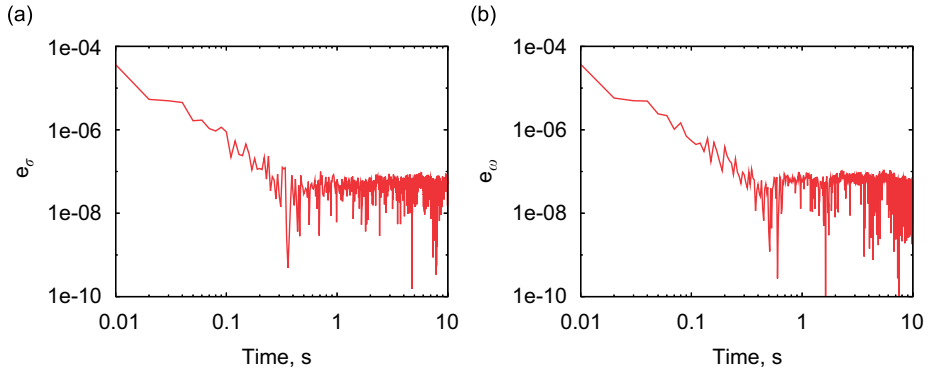


Fig. 3. Time history of the error on the real (a) and imaginary (b) part of the eigenvalue of a damped, single degree of freedom, oscillating system.

numerically compute the covariance matrices, and do not significantly deteriorate even when the covariance coefficients tend to zero; they rather level down to the value reached when the time histories practically vanish.

### 3.3. Three masses problem

The problem, illustrated in Fig. 4, consists of three unit masses, constrained by three linear springs and dampers, whose stiffness and damping matrices are given by Eqs. (48) and (49)

$$\mathbf{K} = \begin{bmatrix} k_1 + k_2 & -k_2 & 0 \\ -k_2 & k_2 + k_3 & -k_3 \\ 0 & -k_3 & k_3 \end{bmatrix} = \begin{bmatrix} 2 & -1 & 0 \\ -1 & 2 & -1 \\ 0 & -1 & 1 \end{bmatrix}, \tag{48}$$

$$\mathbf{C} = \begin{bmatrix} c_1 + c_2 & -c_2 & 0 \\ -c_2 & c_2 + c_3 & -c_3 \\ 0 & -c_3 & c_3 \end{bmatrix} = \begin{bmatrix} 0.11 & -0.01 & 0.00 \\ -0.01 & 1.01 & -1.00 \\ 0.00 & -1.00 & 1.00 \end{bmatrix}, \tag{49}$$

which correspond to unit springs, $k_1 = k_2 = k_3 = 1$ and dampers with $c_1 = 0.1$, $c_2 = 0.01$ and $c_3 = 1.0$ damping coefficients. The masses are only allowed to move along one direction, so the system has three degrees of freedom. The damping matrix has been designed to yield rather different damping values for the three modes that characterize the system, so that system identification becomes critical. The eigenvalues of the system are illustrated in Table 1.

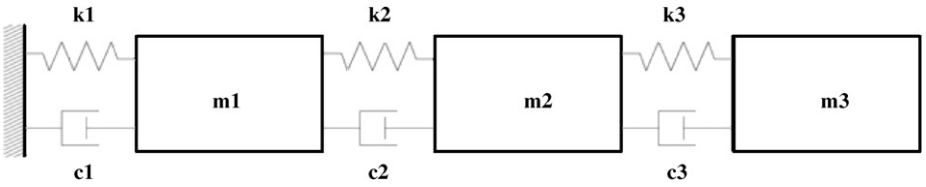


Fig. 4. Three masses problem layout.

Table 1
Eigenvalues of the three masses problem; $\omega_0 = |\lambda|$, $\xi = -\mathrm{Re}(\lambda)/\omega_0$

| Eigenvalue | Re($\lambda$) (rad/s) | Im($\lambda$) (rad/s) | $\xi$ (adim) | $\omega_0$ (rad/s) |
|---|---|---|---|---|
| 1 | −0.015059 | 0.448423 | 0.033563 | 0.448676 |
| 2 | −0.904913 | 1.157122 | 0.616029 | 1.468945 |
| 3 | −0.140028 | 1.510790 | 0.092290 | 1.517266 |

The system of differential equations is integrated in time with a time step of 0.01 s. As clearly shown by Fig. 5, the effects related to the highly damped eigenvalues quickly disappear leaving just an oscillation on the frequency of the slow, lightly damped, first eigenvalue.

Table 2 shows the real and imaginary part of each eigenvalue identified by using the different techniques presented, while Table 3 gives the relative errors made by the identification techniques associated with each eigenvalue. Using the exact value of the acceleration of the masses at each time step, the estimates obtained with both techniques, Eqs. (20) and (21), are of high quality with an error on the real and imaginary parts of the eigenvalues which is below $1.5e-10$ (see first row of Table 3). The complex eigenvectors, illustrated in Fig. 6, also show a very low average relative error, below $1.0e-8$. Using a second order, centered finite difference approximation to compute the acceleration signal from the computed position and velocity, the error in the estimated eigenvectors increases, and a difference appears between the two different formulas (second and third line in Tables 2 and 3). Estimates obtained with Eq. (20) are always between two and three orders of magnitude more accurate than those obtained using Eq. (21). This is related to the fact that the covariance matrix $\mathbf{\Sigma}_{\dot{\mathbf{x}}\dot{\mathbf{x}}}$ is more affected by the numerical error introduced by the finite difference formula. The effect of this error is visible in the eigenvector estimate as well, at least for those obtained using Eq. (21). Fig. 6 shows a comparison between the real and the computed eigenvectors in this last case. A significant error appears in the second eigenvector, which is highly damped.

In order to check the robustness of the method, a disturbance is added in terms of a random perturbing force (rpf) applied concurrently to the three bodies. This approach has been preferred to adding a measurement noise, because the velocity and position signal presented in the numerical examples are directly obtained by numerical simulation. In any case, results are expected to be similar to those obtained by considering measurement noise on acceleration signals from experiments. A limit case is presented with input force signal variance $\sigma_{\mathrm{FF}} = 0.1$; lower force levels result in much better quality of the estimated eigensolutions. The resulting time histories of velocity and acceleration during the simulation are shown in Fig. 7, which can be compared to the "clean" case in Fig. 5. With this disturbance, the estimates obtained for the imaginary part of the eigenvalue by Eq. (20) are still acceptable, while the accuracy on the real part is generally poorer, especially on the less damped modes (see Tables 2 and 3). Note that the application of Eq. (21), which directly uses the acceleration signals, produces relative errors of more than 100%, yielding unreliable results. In this case, the filtering effect obtained by the numerical integration limits the impact of the disturbance on the estimated eigenvalues. Since the free response of the system vanishes, the quality of the covariance matrices and of the identification in this last case is largely affected by the duration of the time series, because the disturbance does not vanish and thus the signal to "noise" ratio quickly deteriorates the quality of the estimates.

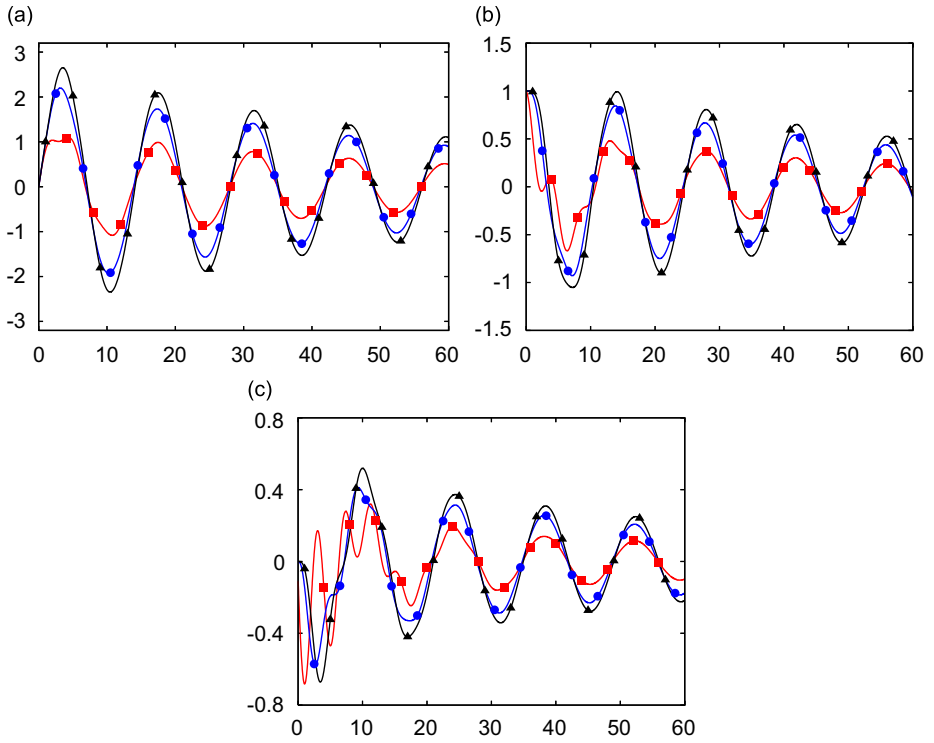


Fig. 5. Time response of the three masses system to an initial perturbation: position (a), velocity (b), and acceleration (c) of mass 1 (■), 2 (•), 3 (▲).

Table 2
Eigenvalues evaluated by the different schemes

| Case | Eig. 1 | | Eig. 2 | | Eig. 3 | |
|---|---|---|---|---|---|---|
| | Re($\lambda$) | Im($\lambda$) | Re($\lambda$) | Im($\lambda$) | Re($\lambda$) | Im($\lambda$) |
| Exact acc. | −0.01506 | 0.4484 | −0.90491 | 1.1571 | −0.14003 | 1.5108 |
| Eq. (20) 2nd acc. | −0.01506 | 0.4484 | −0.90491 | 1.1571 | −0.14002 | 1.5108 |
| Eq. (21) 2nd acc. | −0.01502 | 0.4475 | −0.90204 | 1.1535 | −0.13958 | 1.5060 |
| Eq. (20) + (rpf) | −0.00916 | 0.4517 | −0.82790 | 1.1234 | −0.16375 | 1.5319 |
| Eq. (21) + (rpf) | −0.00521 | 0.4735 | −0.99272 | 3.7192 | −0.00550 | 1.5484 |

Table 3
Relative error on the eigenvalues evaluated by the different schemes

| Case | Eig. 1 | | Eig. 2 | | Eig. 3 | |
|---|---|---|---|---|---|---|
| | Re($\lambda$) | Im($\lambda$) | Re($\lambda$) | Im($\lambda$) | Re($\lambda$) | Im($\lambda$) |
| Exact acc. | 1.5e − 12 | 6.2e − 14 | 3.0e − 11 | 1.5e − 10 | 8.4e − 13 | 1.1e − 11 |
| Eq. (20) 2nd acc. | 3.2e − 06 | 8.4e − 07 | 7.5e − 06 | 1.4e − 05 | 2.4e − 05 | 9.3e − 06 |
| Eq. (21) 2nd acc. | 2.4e − 03 | 2.0e − 03 | 3.2e − 03 | 3.1e − 03 | 3.2e − 03 | 3.1e − 03 |
| Eq. (20) + (rpf) | 3.9e − 01 | 7.2e − 03 | 8.5e − 02 | 2.9e − 02 | 1.7e − 01 | 1.4e − 02 |
| Eq. (21) + (rpf) | 1.3e − 00 | 5.6e − 02 | 9.7e − 02 | 2.2e − 00 | 9.6e − 01 | 1.8e − 02 |

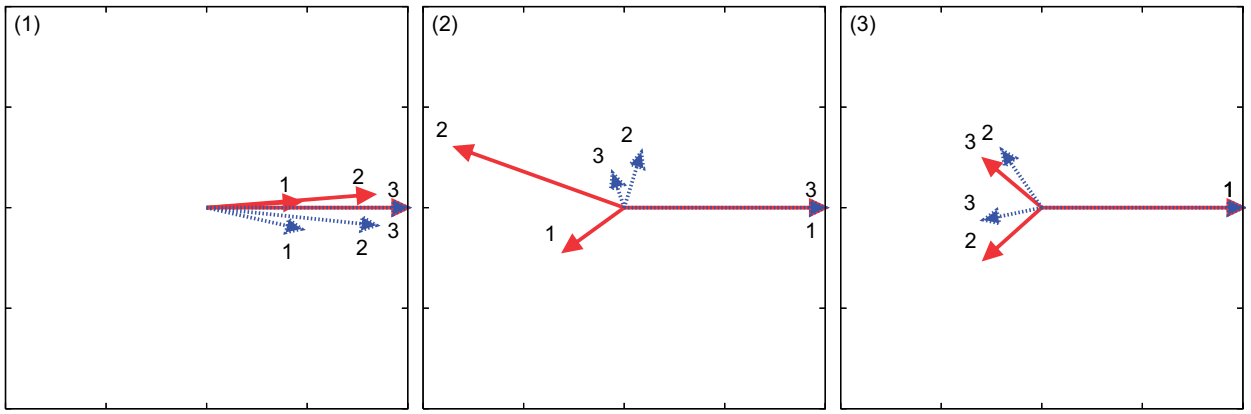


Fig. 6. Comparison between the reference eigenvectors (red, solid lines) and those computed using Eq. (21) using a second-order approximation of acceleration signals (blue, dashed lines).

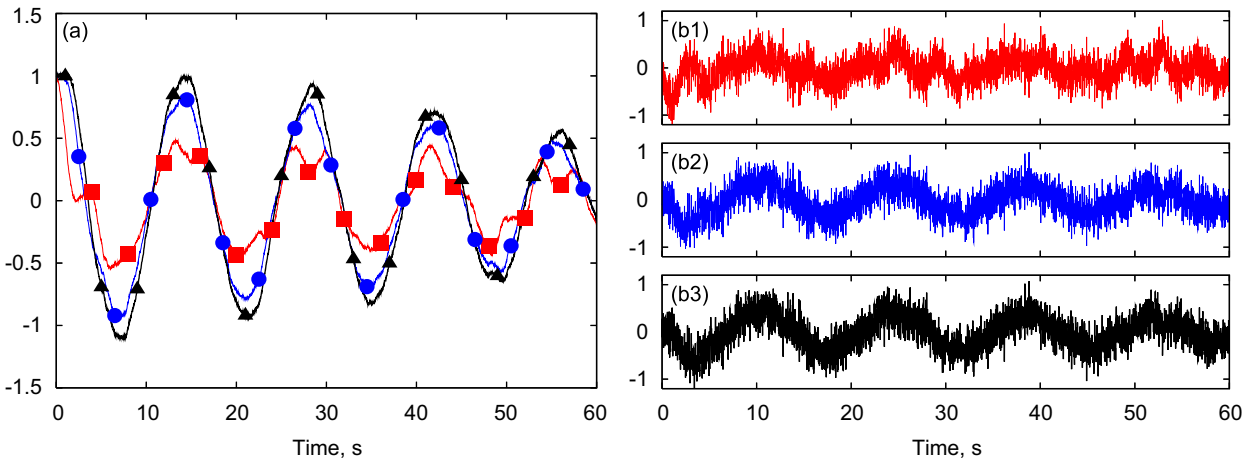


Fig. 7. Time response of the three masses system including random forcing: velocity (a) and acceleration (b 1,2,3) of mass 1 (■), 2, (●) 3 (▲).

Consider now the special case obtained giving the state

$$\mathbf{x} = \begin{Bmatrix} \mathbf{y} \\ \dot{\mathbf{y}} \end{Bmatrix} \tag{50}$$

an initial perturbation with a spatial resolution that exactly corresponds to the arbitrarily chosen $i$th eigenvector of this system

$$\mathbf{x}_0 = \begin{Bmatrix} \mathbf{y}_0 \\ \dot{\mathbf{y}}_0 \end{Bmatrix} = \mathbf{\Phi}_i. \tag{51}$$

As a consequence, the whole system responds only at the frequency corresponding to the excited mode,

$$\mathbf{x} = \mathbf{\Phi}_i e^{\lambda_i t}, \tag{52}$$

$$\dot{\mathbf{x}} = \lambda_i \mathbf{\Phi}_i e^{\lambda_i t}, \tag{53}$$

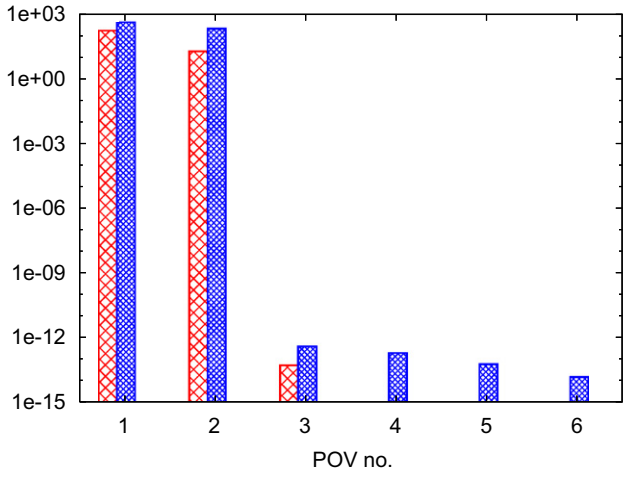


Fig. 8. POVs resulting from POD analysis of the response of the three-masses system when perturbed with a spatial distribution corresponding to the shape of the first mode; $\mathbf{\Sigma}_{\mathbf{yy}}$: bars on the left; $\mathbf{\Sigma}_{\mathbf{xx}}$: bars on the right.

resulting in a spatial coherence of the measures, which makes the covariance matrices

$$\mathbf{\Sigma}_{\mathbf{xx}} = \mathbf{\Phi}_i \mathbf{\Phi}_i^{\mathrm{T}} \frac{1}{\tau} \int_0^{\tau} \mathrm{e}^{2\lambda_i t} \mathrm{d}t, \tag{54}$$

$$\mathbf{\Sigma}_{\mathbf{x}\dot{\mathbf{x}}} = \lambda_i \mathbf{\Phi}_i \mathbf{\Phi}_i^{\mathrm{T}} \frac{1}{\tau} \int_0^{\tau} \mathrm{e}^{2\lambda_i t} \mathrm{d}t, \tag{55}$$

$$\mathbf{\Sigma}_{\dot{\mathbf{x}}\dot{\mathbf{x}}} = \lambda_i^2 \mathbf{\Phi}_i \mathbf{\Phi}_i^{\mathrm{T}} \frac{1}{\tau} \int_0^{\tau} \mathrm{e}^{2\lambda_i t} \mathrm{d}t \tag{56}$$

singular, since $\mathbf{\Phi}_i \mathbf{\Phi}_i^{\mathrm{T}}$ is singular by definition.

In this case, the use of a POD analysis allows to single out the significant signals included in the time histories. However, if the POD is applied to the covariance matrix built using only the position information, namely $\mathbf{\Sigma}_{\mathbf{yy}}$, the resulting POVs are reported in Fig. 8 (bars on the left). The POD seems to indicate that there are two independent signals out of three; however, when Eq. (20) is applied to the time histories of the POMs related to the two non-zero POVs, the problem is still singular. Only applying the POD to the complete (i.e. positions and velocities) state covariance matrix, $\mathbf{\Sigma}_{\mathbf{xx}}$, the correct indication of two significant POMs out of six is obtained; the corresponding POVs are also illustrated in Fig. 8 (bars on the right). The subsequent application of Eq. (20) to the time histories of the two active POMs extracted by the POD allows to correctly identify the eigenvalues corresponding to the modes activated by the perturbation. In conclusion, this approach does not directly deal with spatial resolution by itself, which is rather delegated to prior POD analysis.

## 4. Persistent excitation

In order to overcome the limitations of the free response analysis, similar techniques, based on covariance matrices, can be applied also when a persistent excitation is present. Consider a linear system with the addition of external inputs

$$\dot{\mathbf{x}} = \mathbf{A}\mathbf{x} + \mathbf{B}\mathbf{u}. \tag{57}$$

Eq. (8) is still valid; however, in order to give the correct interpretation of all terms, the effect of the system inputs must be taken into account. Recalling Eq. (5), the derivative of $\mathbf{x}$ is now replaced by that in Eq. (57) to yield the error

$$(\lambda\mathbf{x} - \mathbf{A}\mathbf{x} - \mathbf{B}\mathbf{u})^{\mathrm{T}}\mathbf{\Phi} = \varepsilon. \tag{58}$$

The integral measure of the error becomes

$$J = \lim_{\tau\to\infty} \frac{1}{4\tau} \int_{-\tau}^{\tau} \varepsilon^2 \mathrm{d}t. \tag{59}$$

Applying exactly the same procedure as in Eq. (8), the expression

$$\left( \lim_{\tau\to\infty} \frac{1}{2\tau} \int_{-\tau}^{\tau} (\lambda\mathbf{x} - \mathbf{A}\mathbf{x} - \mathbf{B}\mathbf{u})(\lambda\mathbf{x} - \mathbf{A}\mathbf{x} - \mathbf{B}\mathbf{u})^{\mathrm{T}} \mathrm{d}t \right) \mathbf{\Phi} = \mathbf{0} \tag{60}$$

results from the minimization of $J$ in Eq. (59). Integration over the sampling interval $[-\tau, \tau]$ for $\tau \to \infty$ yields

$$\left(\lambda^2 \mathbf{\Sigma}_{\mathbf{xx}} - \lambda(\mathbf{A}\mathbf{\Sigma}_{\mathbf{xx}} + \mathbf{B}\mathbf{\Sigma}_{\mathbf{ux}} + \mathbf{\Sigma}_{\mathbf{xx}}\mathbf{A}^{\mathrm{T}} + \mathbf{\Sigma}_{\mathbf{xu}}\mathbf{B}^{\mathrm{T}}) + \mathbf{A}\mathbf{\Sigma}_{\mathbf{xx}}\mathbf{A}^{\mathrm{T}} + \mathbf{A}\mathbf{\Sigma}_{\mathbf{xu}}\mathbf{B}^{\mathrm{T}} + \mathbf{B}\mathbf{\Sigma}_{\mathbf{ux}}\mathbf{A}^{\mathrm{T}} + \mathbf{B}\mathbf{\Sigma}_{\mathbf{uu}}\mathbf{B}^{\mathrm{T}}\right)\mathbf{\Phi} = \mathbf{0}. \tag{61}$$

Comparing Eqs. (8) and (61) one can observe that, by analogy

$$\mathbf{\Sigma}_{\dot{\mathbf{x}}\dot{\mathbf{x}}} = \mathbf{A}\mathbf{\Sigma}_{\mathbf{xx}}\mathbf{A}^{\mathrm{T}} + \mathbf{A}\mathbf{\Sigma}_{\mathbf{xu}}\mathbf{B}^{\mathrm{T}} + \mathbf{B}\mathbf{\Sigma}_{\mathbf{ux}}\mathbf{A}^{\mathrm{T}} + \mathbf{B}\mathbf{\Sigma}_{\mathbf{uu}}\mathbf{B}^{\mathrm{T}}, \tag{62}$$

$$\mathbf{\Sigma}_{\dot{\mathbf{x}}\mathbf{x}} + \mathbf{\Sigma}_{\mathbf{x}\dot{\mathbf{x}}} = \mathbf{A}\mathbf{\Sigma}_{\mathbf{xx}} + \mathbf{\Sigma}_{\mathbf{xx}}\mathbf{A}^{\mathrm{T}} + \mathbf{B}\mathbf{\Sigma}_{\mathbf{ux}} + \mathbf{\Sigma}_{\mathbf{xu}}\mathbf{B}^{\mathrm{T}}. \tag{63}$$

### 4.1. White noise

To obtain a persistent excitation, consider as input signal a white noise, namely a signal whose covariance matrix is

$$\mathbf{K}_{\mathbf{uu}} = \lim_{\tau\to\infty} \frac{1}{\tau} \int_{-\tau}^{\tau} \mathbf{u}(v)\mathbf{u}^{\mathrm{T}}(v+t)\,\mathrm{d}v \tag{64}$$

$$= \mathbf{W}\delta(t), \tag{65}$$

where $\mathbf{W}$ is the noise intensity matrix, and $\delta(t)$ is Dirac's delta distribution:

$$\int_{-\infty}^{\infty} \delta(t)\,\mathrm{d}t = 1, \tag{66}$$

$$\int_{-\infty}^{\infty} f(t)\delta(t)\,\mathrm{d}t = f(0). \tag{67}$$

In this special case, the covariance matrix computed with no time shift, i.e. for $t = 0$, is not defined as a function; however, with a small abuse of mathematical notation, it is possible to define

$$\mathbf{\Sigma}_{\mathbf{uu}} \stackrel{\mathrm{def}}{=} \lim_{t\to 0} \mathbf{W}\delta(t) = \mathbf{W}\delta_L, \tag{68}$$

where $\delta_L = \delta(0)$ in theory means $+\infty$, but never needs to be practically evaluated, as illustrated in the following.

In this case the cross-covariance between the state vector and the input signal becomes exactly equal to

$$\mathbf{\Sigma}_{\mathbf{xu}} = \tfrac{1}{2}\mathbf{B}\mathbf{W}. \tag{69}$$

Eq. (61), which is valid only in the limit sense, then becomes

$$\lambda^2 \mathbf{\Sigma}_{\mathbf{xx}} - \lambda(\mathbf{A}\mathbf{\Sigma}_{\mathbf{xx}} + \mathbf{\Sigma}_{\mathbf{xx}}\mathbf{A}^{\mathrm{T}} + \mathbf{B}\mathbf{W}\mathbf{B}^{\mathrm{T}}) + \mathbf{A}\mathbf{\Sigma}_{\mathbf{xx}}\mathbf{A}^{\mathrm{T}} + \tfrac{1}{2}\mathbf{A}\mathbf{B}\mathbf{W}\mathbf{B}^{\mathrm{T}} + \tfrac{1}{2}\mathbf{B}\mathbf{W}\mathbf{B}^{\mathrm{T}}\mathbf{A}^{\mathrm{T}} + \mathbf{B}\mathbf{W}\mathbf{B}^{\mathrm{T}}\delta_L = \mathbf{0} \tag{70}$$

while Eqs. (62) and (63) become

$$\mathbf{\Sigma}_{\dot{\mathbf{x}}\dot{\mathbf{x}}} = \mathbf{A}\mathbf{\Sigma}_{\mathbf{xx}}\mathbf{A}^{\mathrm{T}} + \tfrac{1}{2}\mathbf{A}\mathbf{B}\mathbf{W}\mathbf{B}^{\mathrm{T}} + \tfrac{1}{2}\mathbf{B}\mathbf{W}\mathbf{B}^{\mathrm{T}}\mathbf{A}^{\mathrm{T}} + \mathbf{B}\mathbf{W}\mathbf{B}^{\mathrm{T}}\delta_L, \tag{71}$$

$$\mathbf{\Sigma}_{\dot{\mathbf{x}}\mathbf{x}} + \mathbf{\Sigma}_{\mathbf{x}\dot{\mathbf{x}}} = \mathbf{A}\mathbf{\Sigma}_{\mathbf{xx}} + \mathbf{\Sigma}_{\mathbf{xx}}\mathbf{A}^{\mathrm{T}} + \mathbf{B}\mathbf{W}\mathbf{B}^{\mathrm{T}}. \tag{72}$$

In this case also $\mathbf{\Sigma}_{\dot{\mathbf{x}}\dot{\mathbf{x}}}$ cannot be defined as a function, so it is necessary to see it as

$$\mathbf{\Sigma}_{\dot{\mathbf{x}}\dot{\mathbf{x}}} \stackrel{\mathrm{def}}{=} \lim_{t\to 0} \mathbf{K}_{\dot{\mathbf{x}}\dot{\mathbf{x}}}(t) \tag{73}$$

and

$$\mathbf{K}_{\dot{\mathbf{x}}\dot{\mathbf{x}}}(t) = \lim_{\tau\to\infty}\frac{1}{2\tau}\int_{-\tau}^{\tau}\dot{\mathbf{x}}(v)\dot{\mathbf{x}}^{\mathrm{T}}(v+t)\,\mathrm{d}v. \tag{74}$$

When the signals are stationary, as they are in this case since the system is excited by a stationary white noise, exploiting Eq. (24) in Eq. (72) gives the well known Lyapunov's algebraic equation for the computation of state covariances[3] [19]

$$\mathbf{A}\boldsymbol{\Sigma}_{\mathbf{xx}} + \boldsymbol{\Sigma}_{\mathbf{xx}}\mathbf{A}^{\mathrm{T}} + \mathbf{B}\mathbf{W}\mathbf{B}^{\mathrm{T}} = \mathbf{0}. \tag{75}$$

Remembering that $\boldsymbol{\Sigma}_{\mathbf{x}\dot{\mathbf{x}}} = \boldsymbol{\Sigma}_{\dot{\mathbf{x}}\mathbf{x}}^{\mathrm{T}}$, Eq. (72) allows to infer

$$\boldsymbol{\Sigma}_{\mathbf{x}\dot{\mathbf{x}}} = \boldsymbol{\Sigma}_{\mathbf{xx}}\mathbf{A}^{\mathrm{T}} + \tfrac{1}{2}\mathbf{B}\mathbf{W}\mathbf{B}^{\mathrm{T}}. \tag{76}$$

The matrix equations obtained so far can be used to identify the state matrix of the observed system.

### 4.2. Measured excitation

When the time history of the input signal $\mathbf{u}$ is known, which means that the covariance $\mathbf{W}$ of the excitation is known as well, one can use the definition of the input-output covariance $\boldsymbol{\Sigma}_{\mathbf{xu}}$ to estimate matrix $\mathbf{B}$

$$\boldsymbol{\Sigma}_{\mathbf{xu}} = \tfrac{1}{2}\mathbf{B}\mathbf{W} \Rightarrow \mathbf{B} = 2\boldsymbol{\Sigma}_{\mathbf{xu}}\mathbf{W}^{-1}, \tag{77}$$

and then matrix $\mathbf{A}$ from a simple elaboration of the transpose of Eq. (76)

$$\mathbf{A} = (\boldsymbol{\Sigma}_{\dot{\mathbf{x}}\mathbf{x}} - 2\boldsymbol{\Sigma}_{\mathbf{xu}}\mathbf{W}^{-1}\boldsymbol{\Sigma}_{\mathbf{ux}})\boldsymbol{\Sigma}_{\mathbf{xx}}^{-1}. \tag{78}$$

### 4.3. Unknown excitation

In many cases of practical interest, it may be reasonably assumed that the applied disturbance is a white noise without any additional information on the time history of the input signals. Consider Eq. (76) and use it to replace $\mathbf{B}\mathbf{W}\mathbf{B}^{\mathrm{T}}$ in Eq. (75)

$$\mathbf{A}\boldsymbol{\Sigma}_{\mathbf{xx}} - \boldsymbol{\Sigma}_{\mathbf{xx}}\mathbf{A}^{\mathrm{T}} + \boldsymbol{\Sigma}_{\mathbf{x}\dot{\mathbf{x}}} - \boldsymbol{\Sigma}_{\dot{\mathbf{x}}\mathbf{x}} = \mathbf{0}, \tag{79}$$

where $\boldsymbol{\Sigma}_{\mathbf{x}\dot{\mathbf{x}}} = \boldsymbol{\Sigma}_{\dot{\mathbf{x}}\mathbf{x}}^{\mathrm{T}}$ and $\boldsymbol{\Sigma}_{\dot{\mathbf{x}}\mathbf{x}}^{\mathrm{T}} = -\boldsymbol{\Sigma}_{\dot{\mathbf{x}}\mathbf{x}}$ have been exploited. This equation is skew-symmetric, and can be used to infer information about the state matrix $\mathbf{A}$ given the covariances. It actually contains $n(n-1)/2$ equations in the $n^2$ unknowns represented by the coefficients of matrix $\mathbf{A}$, so it is not sufficient by itself to determine the unknown matrix.

Consider now

$$\boldsymbol{\Sigma}_{\dot{\mathbf{x}}\mathbf{x}} = \boldsymbol{\Sigma}_{\mathbf{x}\dot{\mathbf{x}}}^{\mathrm{T}} = \mathbf{A}\boldsymbol{\Sigma}_{\mathbf{xx}} + \tfrac{1}{2}\mathbf{B}\mathbf{W}\mathbf{B}^{\mathrm{T}} \tag{80}$$

and use it along with Eq. (76) to eliminate the first two occurrences of $\mathbf{B}\mathbf{W}\mathbf{B}^{\mathrm{T}}$ from Eq. (71); use Eq. (72) along with Eq. (68) to eliminate $\mathbf{B}\mathbf{W}\mathbf{B}^{\mathrm{T}}\delta_L$ as well. Eq. (71) becomes:

$$\mathbf{A}\boldsymbol{\Sigma}_{\mathbf{xx}}\mathbf{A}^{\mathrm{T}} - \mathbf{A}(\boldsymbol{\Sigma}_{\mathbf{x}\dot{\mathbf{x}}} - \delta_L\boldsymbol{\Sigma}_{\mathbf{xx}}) - (\boldsymbol{\Sigma}_{\dot{\mathbf{x}}\mathbf{x}} - \delta_L\boldsymbol{\Sigma}_{\mathbf{xx}})\mathbf{A}^{\mathrm{T}} + \boldsymbol{\Sigma}_{\dot{\mathbf{x}}\dot{\mathbf{x}}} = \mathbf{0}. \tag{81}$$

Eq. (81) represents a second-order algebraic equation in matrix $\mathbf{A}$ which is based on the covariance and cross-covariance matrices of the measurements $\mathbf{x}$ and their derivatives. It is symmetric, so it actually contains the remaining $n(n+1)/2$ equations that are necessary to determine all the coefficients of matrix $\mathbf{A}$.

An asymptotic analysis of Eq. (81) shows that it is dominated by the terms multiplied by $\delta_L$; this term is also implicitly contained in $\boldsymbol{\Sigma}_{\dot{\mathbf{x}}\dot{\mathbf{x}}}$, so when the analytical covariances are considered, for a true, i.e. infinite band,

[3]Note, however, that in this case the equation must be seen in a light that differs from the usual interpretation: the unknown is now matrix $\mathbf{A}$. The essential difference is the lack of symmetry of matrix $\mathbf{A}$, while the covariance matrix is symmetric by definition. As a consequence, Eq. (75) is symmetric but the unknown is not, so it is under-determined.

white noise, it degenerates into

$$\mathbf{A}\boldsymbol{\Sigma}_{\mathbf{xx}} + \boldsymbol{\Sigma}_{\mathbf{xx}}\mathbf{A}^{\mathrm{T}} + \lim_{t\to 0}\frac{1}{\delta(t)}\mathbf{K}_{\dot{\mathbf{x}}\dot{\mathbf{x}}}(t) = \mathbf{0}, \tag{82}$$

where the limit exists and is finite. Eq. (82) is again the well-known Lyapunov's algebraic equation.

The union of the skew-symmetric Eq. (79) and of the symmetric Eq. (81), or of the corresponding asymptotic one (82), yields a system of equations that is consistent. If Eq. (82) can be considered, the system is linear; otherwise, a weakly quadratic problem results, where the importance of the quadratic term grows as the noise bandwidth decreases.

In conclusion, considering an unknown linear system subjected to white random noise in input, using the information contained in the covariance matrices, through Eqs. (79), (81), the state matrix can be identified. This very interesting result, to the authors' knowledge, has never been shown before.

### 4.4. Band limited white noise

A term that goes to infinity, $\delta_L$, appears in Eq. (81). This is due to the fact that the covariance of an ideal white noise goes to infinity, so a process like that is not physically realizable. However, it can be approximated by what is usually called a *wide band white noise with exponential correlation* [15], defined by a covariance matrix

$$\mathbf{K}_{\mathbf{uu}}(t) = \mathbf{W}\frac{\alpha}{2}\mathrm{e}^{-\alpha|t|}, \tag{83}$$

where $\alpha$ is the band limit [15]. This process becomes a white noise when $\alpha \to \infty$. The variance between the system state and the input signal is

$$\begin{aligned}\boldsymbol{\Sigma}_{\mathbf{xu}} &= \lim_{\tau\to\infty}\frac{1}{2\tau}\int_{-\tau}^{\tau}\int_{-\infty}^{\infty}\mathrm{e}^{\mathbf{A}v}\mathbf{B}\mathbf{u}(t-v)\mathbf{u}^{\mathrm{T}}(t)\,\mathrm{d}v\,\mathrm{d}t\\ &= \int_{-\infty}^{\infty}\mathrm{e}^{\mathbf{A}v}\mathbf{B}\mathbf{W}\frac{\alpha}{2}\mathrm{e}^{-\alpha|v|}\,\mathrm{d}v\\ &= \frac{\alpha}{2}\left(\int_{-\infty}^{\infty}\mathrm{e}^{\mathbf{A}v-\mathbf{I}\alpha|v|}\,\mathrm{d}v\right)\mathbf{B}\mathbf{W}.\end{aligned}$$

If the band limit is large enough compared to the characteristic frequencies of the system under analysis, the term under the integral expression can be approximated by $\mathrm{e}^{-\alpha|v|}$, so the covariance becomes

$$\boldsymbol{\Sigma}_{\mathbf{xu}} \approx \tfrac{1}{2}\mathbf{B}\mathbf{W}, \tag{84}$$

which corresponds to the expression obtained for the white noise, Eq. (69). The covariance matrix of the band limited noise for $t = 0$ becomes equal to

$$\boldsymbol{\Sigma}_{\mathbf{uu}} = \mathbf{W}\frac{\alpha}{2} = \mathbf{W}\delta_F, \tag{85}$$

where the value of $\delta_F$ is now limited by the bandwidth $\alpha$ of the noise.

In all the numerical examples presented in the following section the white noise has been simulated using a set of normally distributed random numbers generated at each time step by the Matlab function `randn`. A simple relation between the discrete and the continuous domain shows that the noise bandwidth is $2/\Delta t$, and thus $\delta_F = 1/\Delta t$. These values have been confirmed by simple numerical experiments, where the power spectral density of the generated noise has been computed and evaluated.

### 4.5. Numerical solution for the unknown excitation case

In the most general case, when a wide band white noise is considered as input, and the noise input is unknown, the system of matrix equations

$$U(\mathbf{A}\boldsymbol{\Sigma}_{\mathbf{xx}}\mathbf{A}^{\mathrm{T}} - \mathbf{A}(\boldsymbol{\Sigma}_{\mathbf{x}\dot{\mathbf{x}}} - \delta_F\boldsymbol{\Sigma}_{\mathbf{xx}}) - (\boldsymbol{\Sigma}_{\dot{\mathbf{x}}\mathbf{x}} - \delta_F\boldsymbol{\Sigma}_{\mathbf{xx}})\mathbf{A}^{\mathrm{T}} + \boldsymbol{\Sigma}_{\dot{\mathbf{x}}\dot{\mathbf{x}}}) = U(\mathbf{0})$$

$$L(\mathbf{A}\boldsymbol{\Sigma}_{\mathbf{xx}} - \boldsymbol{\Sigma}_{\mathbf{xx}}\mathbf{A}^{\mathrm{T}} + \boldsymbol{\Sigma}_{\mathbf{x}\dot{\mathbf{x}}} - \boldsymbol{\Sigma}_{\dot{\mathbf{x}}\mathbf{x}}) = L(\mathbf{0}). \tag{86}$$

must be solved, where operators $U(\cdot)$ and $L(\cdot)$, respectively, return the upper and the strictly lower triangular parts of the argument. The problem is in general nonlinear; the solution can be obtained using a Newton-like iterative numerical method. For conciseness, the problem of Eq. (86) is rewritten as

$$U(\mathbf{A}\mathbf{S}\mathbf{A}^{\mathrm{T}} - \mathbf{A}\mathbf{R} - \mathbf{R}^{\mathrm{T}}\mathbf{A}^{\mathrm{T}} + \mathbf{Q}) = U(\mathbf{0})$$

$$L(\mathbf{A}\mathbf{S} - \mathbf{S}\mathbf{A}^{\mathrm{T}} + \mathbf{P}) = L(\mathbf{0}), \tag{87}$$

where

$$\mathbf{S} = \boldsymbol{\Sigma}_{\mathbf{xx}}, \tag{88}$$

$$\mathbf{R} = \boldsymbol{\Sigma}_{\mathbf{x}\dot{\mathbf{x}}} - \delta_F\boldsymbol{\Sigma}_{\mathbf{xx}}, \tag{89}$$

$$\mathbf{Q} = \boldsymbol{\Sigma}_{\dot{\mathbf{x}}\dot{\mathbf{x}}}, \tag{90}$$

$$\mathbf{P} = \boldsymbol{\Sigma}_{\mathbf{x}\dot{\mathbf{x}}} - \boldsymbol{\Sigma}_{\dot{\mathbf{x}}\mathbf{x}}. \tag{91}$$

After indicating with

$$u_{ij} = a_{ik}s_{kh}a_{jh} - a_{ik}r_{kj} - r_{ki}a_{jk} + q_{ij} = 0 \tag{92}$$

$$l_{ij} = a_{ik}s_{kj} - s_{ik}a_{jk} + p_{ij}, \tag{93}$$

the generic equations from the symmetric ($u_{ij}$, $j \geqslant i$) and the skew-symmetric ($l_{ij}$, $j < i$) problems, respectively, the Jacobian matrix can be analytically computed as

$$\frac{\partial u_{ij}}{\partial a_{mn}} = \delta_{im}s_{nh}a_{jh} + \delta_{jm}a_{ik}s_{kn} - \delta_{im}r_{nj} - \delta_{jm}r_{ni}, \tag{94}$$

$$\frac{\partial l_{ij}}{\partial a_{mn}} = \delta_{im}s_{nj} - \delta_{jm}s_{in}, \tag{95}$$

where $\delta_{ij}$ is Kronecker's operator, and implicit summation is assumed over repeated subscripts.

The problem of selecting the "right" solution of the nonlinear problem is yet to be solved; however, in the numerical cases addressed so far this point does not appear to be critical. The same applies to the initial guess of matrix $\mathbf{A}$. The skew-symmetric equation (79) is not required if a second-order model is enforced. In fact, the typical state-space representation of second-order structural problems, where

$$\mathbf{x} = \begin{Bmatrix} \mathbf{y} \\ \mathbf{z} \end{Bmatrix} \tag{96}$$

yields exactly $n(n+1)/2$ unknowns, because matrix $\mathbf{A}$ can be partitioned as

$$\mathbf{A} = \begin{bmatrix} \mathbf{0} & \mathbf{D} \\ \mathbf{A}_{21} & \mathbf{A}_{22} \end{bmatrix}, \tag{97}$$

where $\mathbf{D}$ is a diagonal matrix that contains the scale factors between the derivatives of the positions, $\dot{\mathbf{y}}$, and the pseudo-velocities $\mathbf{z}$, typically equal to the identity matrix $\mathbf{I}$ when $\mathbf{z} = \dot{\mathbf{y}}$.

It appears that any linear combination of Eqs. (79) and (81) represents a general, non-symmetric algebraic Riccati-like[4] equation. The analytical solution of simple cases presented in the following seems to indicate the presence of a reflection axis for the eigenvalues of the two solutions of matrix $\mathbf{A}$, crossing the real axis at $-\delta_F$ and parallel to the imaginary axis. This suggests that some shift technique, capable of bringing the reflection plane onto the imaginary axis, could turn the problem into Hamiltonian form, and thus naturally allow to select the stable solution by using standard techniques for algebraic Riccati equations. However, this direction needs further investigation.

[4]It is not an algebraic Riccati equation because the unknown matrix $\mathbf{A}$ is not symmetric.

The analytical application of the above techniques to a first- and second-order scalar problem, and their numerical application to the three masses problem, is illustrated to clarify their properties.

### 4.6. Scalar, first-order problem

Consider the scalar problem

$$\dot{y} = \lambda y + \beta u. \tag{98}$$

The covariance matrix can be computed from Lyapunov's equation (75)

$$\lambda\sigma_{yy} + \sigma_{yy}\lambda + \beta^2 w = 0, \tag{99}$$

resulting in

$$\sigma_{yy} = -\frac{\beta^2 w}{2}\frac{1}{\lambda}. \tag{100}$$

By definition, $\sigma_{y\dot{y}} = 0$, while the covariance of $\dot{y}$ is

$$\begin{aligned}\sigma_{\dot{y}\dot{y}} &= \lambda^2\sigma_{yy} + 2\frac{1}{2}\lambda\beta^2 w + \beta^2 w\delta_F \\ &= \frac{\beta^2 w}{2}(\lambda + 2\delta_F).\end{aligned} \tag{101}$$

#### 4.6.1. Unknown excitation

Eq. (81) yields

$$-a^2\frac{\beta^2 w}{2}\frac{1}{\lambda} - 2a\delta_F\frac{\beta^2 w}{2}\frac{1}{\lambda} + \frac{\beta^2 w}{2}(\lambda + 2\delta_F) = 0, \tag{102}$$

where $a$ is the unknown coefficient. It results from the solution of the second-order polynomial equation

$$a^2 + 2\delta_F a - \lambda(\lambda + 2\delta_F) = 0, \tag{103}$$

whose roots are

$$\begin{aligned}a &= -\delta_F \pm \sqrt{\delta_F^2 + \lambda(\lambda + 2\delta_F)}, \\ &= -\delta_F \pm \sqrt{(\lambda + \delta_F)^2}, \\ &= \begin{cases}\lambda \\ -(\lambda + 2\delta_F)\end{cases}.\end{aligned} \tag{104}$$

The first one is the "right" root, while the other, which tends to $-\infty$ according to the ratio between the noise bandwidth and the system eigenvalue, is essentially meaningless. In fact, when using the asymptotic equation (82)

$$-2a\frac{\beta^2 w}{2}\frac{1}{\lambda} + \beta^2 w = 0, \tag{105}$$

the correct system root is obtained directly.

#### 4.6.2. Measured excitation

If $u$ is measured, and thus $w$ is known, Eq. (77) yields

$$\begin{aligned}b &= 2\left(\frac{1}{2}\beta w\right)\frac{1}{w} \\ &= \beta,\end{aligned} \tag{106}$$

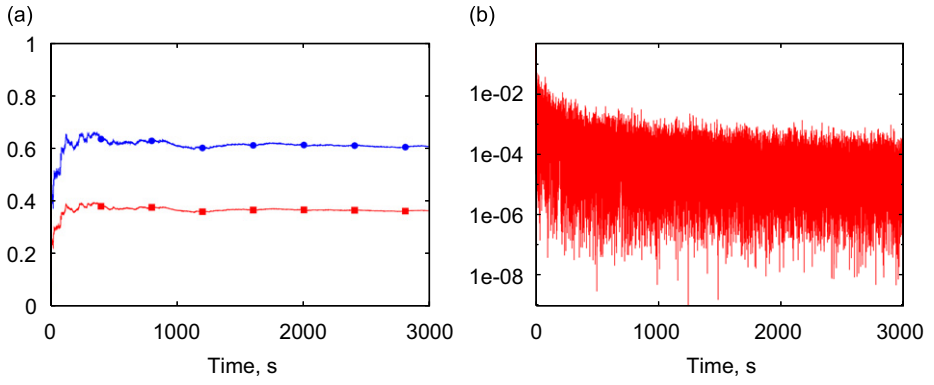


Fig. 9. Time history of covariances for the single dof scalar case: $\Sigma_{xx}$ (a, ■), $\Sigma_{xu}$ (a, •), $\Sigma_{\dot{x}x}$ (b).

while Eq. (78) yields

$$a = \left(0 - 2\left(\frac{1}{2}\beta w\right)\frac{1}{w}\left(\frac{1}{2}\beta w\right)\right)\left(-\lambda\frac{2}{\beta^2 w}\right) = \lambda. \tag{107}$$

A first numerical application has been made on this very simple system. In this case $\lambda = -2$ and $\beta = 1.2$. The system is integrated numerically with a time step of 0.01 s. Fig. 9(a) shows how the state covariance and the cross-covariance between the state and the input converge toward an almost constant value. At least a time of 1000 s is necessary to obtain a significant stabilization in the covariances. However, the analysis of Fig. 9(b) gives an indication about the non-perfect "whiteness" of the input noise. In fact, the cross-covariance between the derivative of the state and the state itself must go to zero. The figure shows that the trend is correct; however, after the initial times, the values seem to reach a plateau. At the same time the measured power spectrum of the noise between 0 and the band limit is far from being regular (either similar to a quadratic decay, as the one associated with the exponential correlation or to a uniform value as the one associated with a band limited white noise [15]). The resulting relative errors in the identified values of $\lambda$ and $\beta$ are shown in Fig. 10. The error drops below 5% after 1000 s (and 100,000 steps), and goes around 1% after 3000 s, with a very slow decay. Such a large time window is taken just to show that the decay of the error after the first time portion is very slow. Interestingly enough, the two relative errors are exactly opposite.

### 4.7. Scalar, second-order problem

Consider the scalar second-order problem

$$m\ddot{y} + c\dot{y} + ky = f \tag{108}$$

cast in first-order form

$$\begin{Bmatrix} \dot{y} \\ \ddot{y} \end{Bmatrix} = \begin{bmatrix} 0 & 1 \\ -k/m & -c/m \end{bmatrix} \begin{Bmatrix} y \\ \dot{y} \end{Bmatrix} + \begin{bmatrix} 0 \\ 1/m \end{bmatrix} f. \tag{109}$$

From Lyapunov's equation and from the definitions of the covariances

$$\sigma_{yy} = \frac{w}{2ck}, \tag{110}$$

$$\sigma_{y\dot{y}} = 0, \tag{111}$$

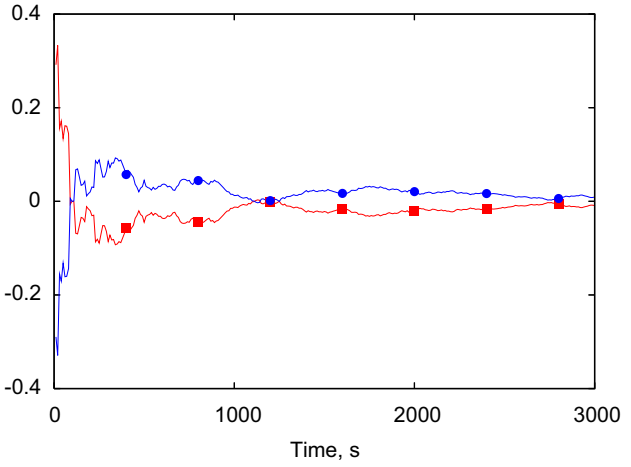


Fig. 10. Time history of the identification error for the single dof scalar case: $\lambda$ (■), $\beta$ (•).

$$\sigma_{\dot{y}\dot{y}} = \frac{w}{2cm}, \tag{112}$$

$$\sigma_{\ddot{y}\ddot{y}} = \frac{w}{2m^2}\left(\frac{k}{c} - \frac{c}{m} + 2\delta_F\right), \tag{113}$$

$$\sigma_{\dot{y}\ddot{y}} = 0, \tag{114}$$

$$\sigma_{y\ddot{y}} = -\frac{w}{2cm}, \tag{115}$$

where $w = \sigma_{ff} = w\delta_F$, which yield

$$\mathbf{\Sigma}_{\mathbf{xx}} = \frac{w}{2}\begin{bmatrix} \frac{1}{ck} & 0 \\ 0 & \frac{1}{cm} \end{bmatrix}, \tag{116}$$

$$\mathbf{\Sigma}_{\mathbf{x}\dot{\mathbf{x}}} = \frac{w}{2}\begin{bmatrix} 0 & -\frac{1}{cm} \\ \frac{1}{cm} & 0 \end{bmatrix}, \tag{117}$$

$$\mathbf{\Sigma}_{\dot{\mathbf{x}}\dot{\mathbf{x}}} = \frac{w}{2}\begin{bmatrix} \frac{1}{cm} & 0 \\ 0 & \frac{1}{m^2}\left(\frac{k}{c} - \frac{c}{m} + 2\delta_F\right) \end{bmatrix}. \tag{118}$$

*4.7.1. Unknown excitation*

From Eq. (81), by imposing that matrix $\mathbf{A}$ takes the form

$$\mathbf{A} = \begin{bmatrix} 0 & a_{12} \\ a_{21} & a_{22} \end{bmatrix}, \tag{119}$$

where $a_{11} = 0$ is assumed because matrix $\mathbf{A}$ is the first-order representation of a second-order scalar equation,[5] one obtains

$$a_{12} = 1, \tag{120}$$

$$a_{21} = -\frac{k}{m}, \tag{121}$$

$$a_{22} = \begin{cases} -\dfrac{c}{m}, \\ \dfrac{c}{m} - 2\delta_F \end{cases}. \tag{122}$$

The result of Eq. (120) is expected; however it may not be trivial if, for example, some scaling occurs between the derivatives of the measurements. Eq. (121) yields the exact result for the stiffness-mass ratio; this is also expected. Eq. (122) allows two results; one is the exact value of the damping-mass ratio, while the other is essentially irrelevant. Again it tends to $-\infty$, so it is easily distinguishable from the correct one.

*4.7.2. Measured excitation*

If $f$ is measured, the exact values are obtained for matrices $\mathbf{B}$ and $\mathbf{A}$:

$$\mathbf{B} = 2\begin{bmatrix} \sigma_{yf} \\ \sigma_{\dot{y}f} \end{bmatrix} w^{-1} = 2\begin{bmatrix} 0 \\ \dfrac{w}{2m} \end{bmatrix} w^{-1} = \begin{bmatrix} 0 \\ \dfrac{1}{m} \end{bmatrix}, \tag{123}$$

$$\begin{aligned} \mathbf{A} &= \left( \begin{bmatrix} \sigma_{\dot{y}y} & \sigma_{\dot{y}\dot{y}} \\ \sigma_{\ddot{y}y} & \sigma_{\ddot{y}\dot{y}} \end{bmatrix} - \begin{bmatrix} b_{11} \\ b_{21} \end{bmatrix} \begin{bmatrix} \sigma_{fy} & \sigma_{f\dot{y}} \end{bmatrix} \right) \begin{bmatrix} \sigma_{yy} & \sigma_{y\dot{y}} \\ \sigma_{\dot{y}y} & \sigma_{\dot{y}\dot{y}} \end{bmatrix}^{-1} \\ &= \left( \begin{bmatrix} 0 & \dfrac{w}{2cm} \\ -\dfrac{w}{2cm} & 0 \end{bmatrix} - \begin{bmatrix} 0 & 0 \\ 0 & \dfrac{w}{2m^2} \end{bmatrix} \right) \begin{bmatrix} \dfrac{2ck}{w} & 0 \\ 0 & \dfrac{2cm}{w} \end{bmatrix} \\ &= \begin{bmatrix} 0 & 1 \\ -\dfrac{k}{m} & -\dfrac{c}{m} \end{bmatrix}, \end{aligned} \tag{124}$$

where

$$\sigma_{yf} = m\sigma_{y\ddot{y}} + c\sigma_{y\dot{y}} + k\sigma_{yy} = 0, \tag{125}$$

$$\sigma_{\dot{y}f} = m\sigma_{\dot{y}\ddot{y}} + c\sigma_{\dot{y}\dot{y}} + k\sigma_{\dot{y}y} = \frac{w}{2m} \tag{126}$$

have been exploited.

*4.8. Three masses problem*

Consider now the three masses problem of Fig. 4, already used as a test example in earlier sections. In this cases no analytical solution is sought; only numerical solutions are considered.

*4.8.1. Unknown excitation*

In this case, the computation of the covariance matrices suffers from the quality of the noise that is used to force the system. The method assumes that the unknown excitation is white noise, so the results of the identification may significantly depart from the exact value if the power spectral density of the noise is not uniform.

[5]This is required because Eq. (81) is symmetric, and thus it actually represents $n(n+1)/2$ scalar equations only.

The problem has been solved by numerically computing the solution of Eqs. (81) and (79) directly, by means of Matlab's `fsolve` command. The problem consists in 36 equations with 36 unknowns, and the initial guess consisted in a matrix with the structure

$$\mathbf{A}_0 = \begin{bmatrix} \mathbf{0} & \mathbf{I} \\ \mathbf{0} & \mathbf{0} \end{bmatrix}. \tag{127}$$

The result appears to be quite robust with respect to the initial guess of the solution: in no case the procedure converged to a different solution. Of course, this does not represent a proof, neither of uniqueness nor of stability of the solution; further investigation is required to assess the properties of the equation and of its numerical solution.

Three, almost uncorrelated, band-limited white noise forces with different intensity have been applied to the three masses. The intensity matrix $\mathbf{W}$ is reported in the following equation:

$$\mathbf{W} = \begin{bmatrix} 1.00 & -2.45\text{e}-3 & -8.25\text{e}-4 \\ 2.45\text{e}-3 & 2.00 & 4.88\text{e}-4 \\ -8.25\text{e}-4 & 4.88\text{e}-4 & 0.80 \end{bmatrix}, \tag{128}$$

even thought it has not been used for the identification in the cases presented in the following.

The matrix $\mathbf{A}$ resulting from the numerical solution of the problem obtained by joining the two Eqs. (81), (79) is

$$\mathbf{A} = \begin{bmatrix} -2.244\text{e}-5 & -5.531\text{e}-6 & 8.440\text{e}-6 & 0.999 & -1.541\text{e}-4 & 1.878\text{e}-4 \\ 1.367\text{e}-5 & 3.571\text{e}-6 & -5.320\text{e}-6 & 5.280\text{e}-5 & 1.000 & -1.142\text{e}-4 \\ -3.096\text{e}-6 & -8.920\text{e}-7 & 1.282\text{e}-6 & -1.189\text{e}-5 & -2.099\text{e}-5 & 1.000 \\ -2.040 & 1.069 & -3.919\text{e}-2 & -8.253\text{e}-2 & 1.589\text{e}-2 & -2.217\text{e}-2 \\ 0.991 & -1.983 & 0.988 & -1.236\text{e}-2 & -1.028 & 1.021 \\ -3.021\text{e}-3 & 1.041 & -1.031 & -1.063\text{e}-4 & 1.020 & -1.019 \end{bmatrix},$$

which shows the structure of Eq. (97), with a null $3 \times 3$ matrix in the upper left corner and the identity matrix in the upper right corner. The most significant coefficients of the stiffness and damping matrices are visible too. The convergence in the solution of the nonlinear problem of Eq. (86) is extremely fast, as shown in Fig. 11 where the trend of the norm of the problem residual is shown. In Table 4, the results of the eigensolutions resulting from the matrix identified using covariance matrices after 500 and 3000 s of elapsed time are compared with the exact ones. Table 5 shows analogous results obtained with a classical discrete subspace identification method, N4SID [20], considering a stochastic unknown input. The comparison of the two tables shows that the quality of the results is comparable, with a slight advantage on the method here proposed. The error is generally low for the imaginary part and can be considered acceptable for the real part related to the damping. The error on the computed eigenvectors is shown in Fig. 12.

#### 4.8.2. *Measured excitation*

Using the knowledge of the time history of the input noise, the other form of identification can be adopted, which additionally gives the input matrix $\mathbf{B}$. The error on the computed eigenvalues is presented in Table 6. It can be considered generally acceptable, even thought the real part of the less damped eigenvector has a much higher error, compared with the case of unknown input noise (Table 4). In this case it is interesting to analyze the trends of the errors during the measuring time, shown in Fig. 13. The diagrams clearly show how the errors decrease very quickly in the first 500 s; then a slow decay starts with some spot windows where the error drops. It is believed that this behavior is caused by the non-perfect "whiteness" of the generated noise. Furthermore, it is worth stressing that in this last case the identified matrices $\mathbf{A}$ and $\mathbf{B}$ do not allow to clearly recognize the classical structure of the state space form of second-order systems, like in the case of unknown excitation.

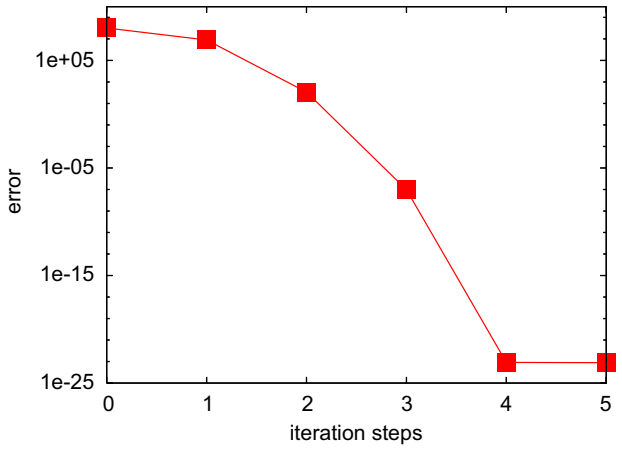


Fig. 11. Residual norm during the solution of the nonlinear problem of Eq. (86).

Table 4
Identified eigenvalues of the three masses problem with the unknown input noise

| Elapsed time (s) | Eig. | Re($\lambda$) (rad/s) | Im($\lambda$) (rad/s) | err. Re($\lambda$) | err. Im($\lambda$) |
|---|---|---|---|---|---|
| 500 | 1 | −0.01237 | 0.4446 | 0.17860 | 8.577e − 3 |
| | 2 | −0.87735 | 1.2473 | 0.03046 | 7.797e − 2 |
| | 3 | −0.11655 | 1.5295 | 0.16767 | 1.238e − 2 |
| 3000 | 1 | −0.01377 | 0.4494 | 0.08537 | 2.126e − 3 |
| | 2 | −0.91287 | 1.1590 | 0.00880 | 1.635e − 3 |
| | 3 | −0.11696 | 1.5207 | 0.16477 | 6.546e − 3 |

Table 5
Identified eigenvalues of the three masses problem with stochastic N4SID

| Elapsed time (s) | Eig. | Re($\lambda$) (rad/s) | Im($\lambda$) (rad/s) | err. Re($\lambda$) | err. Im($\lambda$) |
|---|---|---|---|---|---|
| 500 | 1 | −0.01164 | 0.4464 | 0.2268 | 8.428e − 3 |
| | 2 | −0.92309 | 1.3342 | 0.0200 | 1.530e − 1 |
| | 3 | −0.08687 | 1.4988 | 0.3796 | 7.9621 − 3 |
| 3000 | 1 | −0.01399 | 0.4495 | 0.0706 | 2.419e − 3 |
| | 2 | −0.93806 | 1.2065 | 0.0366 | 4.263e − 3 |
| | 3 | −0.10022 | 1.5341 | 0.2842 | 2.512e − 3 |

The resulting matrix $B$ is

$$\mathbf{B} = \begin{bmatrix} -1.4584\text{e}-1 & -5.9196\text{e}-2 & 1.3117\text{e}-1 \\ -9.2979\text{e}-2 & -5.8983\text{e}-2 & 2.2654\text{e}-1 \\ -1.3850\text{e}-1 & -8.5302\text{e}-2 & 2.1200\text{e}-1 \\ 1.1379\text{e}+0 & -7.3443\text{e}-2 & -4.4223\text{e}-3 \\ 3.6637\text{e}-2 & 9.8293\text{e}-1 & 1.1803\text{e}-1 \\ 7.0270\text{e}-2 & -1.0066\text{e}-3 & 1.1032\text{e}+0 \end{bmatrix},$$

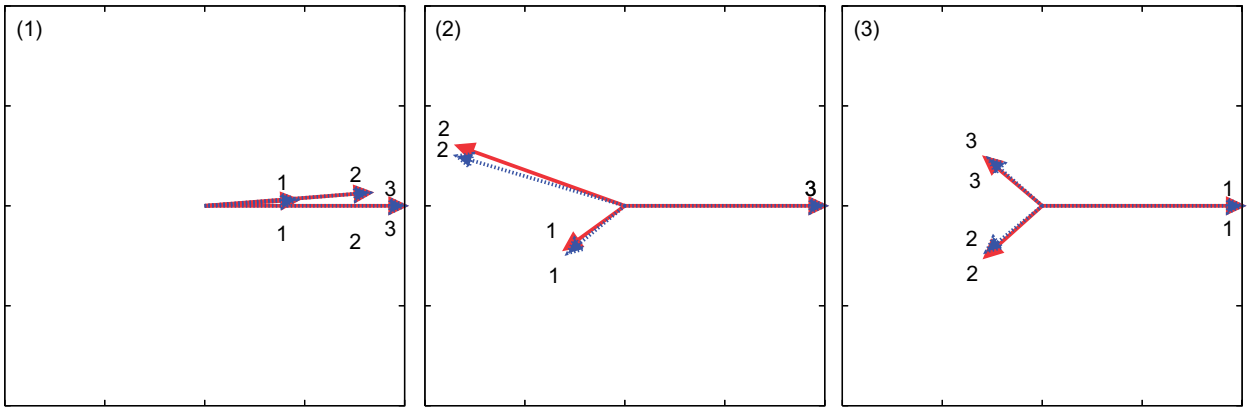


Fig. 12. Comparison between the reference eigenvectors (red, solid lines) and those computed with the unknown noise excitation method (blue, dashed lines).

Table 6
Identified eigenvalues of the three masses problem with measured excitation after 3000 s

| Eigenvalue | Re($\lambda$) (rad/s) | Im($\lambda$) (rad/s) | err. Re($\lambda$) | err. Im($\lambda$) |
|---|---|---|---|---|
| 1 | −0.016627 | 0.44956 | 0.10414 | 2.5459e − 3 |
| 2 | −0.90583 | 1.1765 | 1.0083e − 3 | 1.6753e − 2 |
| 3 | −0.15560 | 1.5101 | 0.1118 | 4.5549e − 4 |

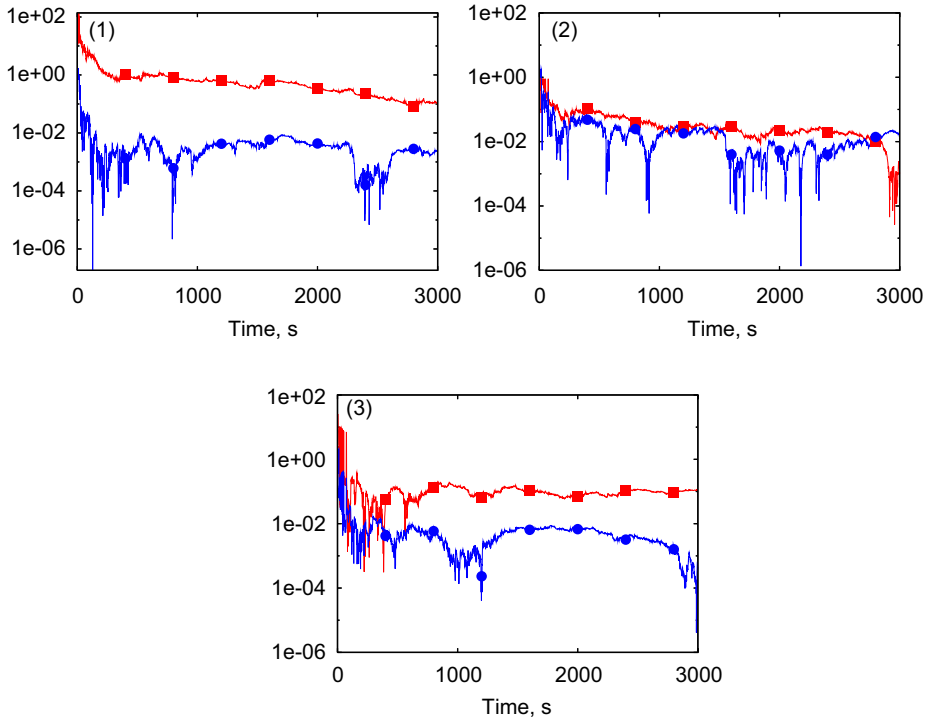


Fig. 13. Relative error on the real and imaginary part of the eigenvalues of the three masses problem, identified using the measured input method: real (■) and imaginary (●) part.

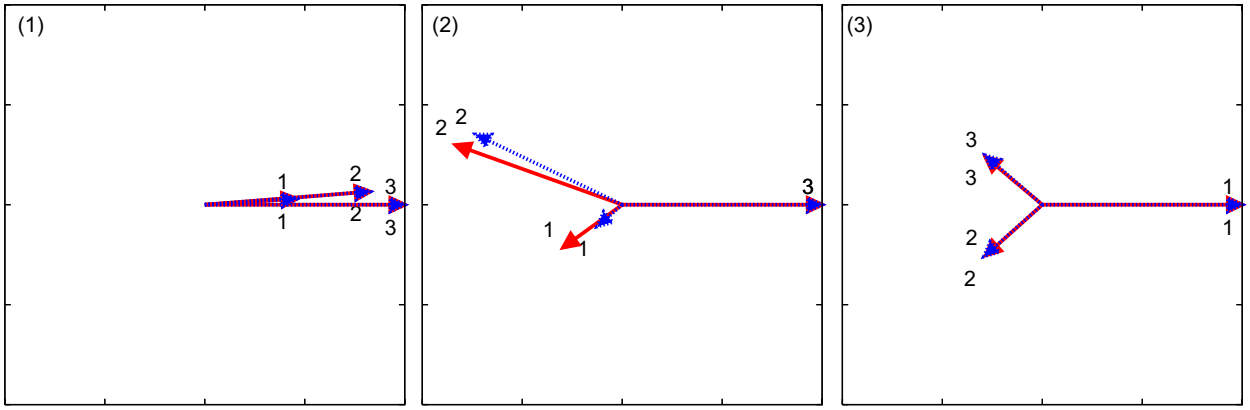


Fig. 14. Comparison between the reference eigenvectors (red, solid lines) and those computed with the measured noise excitation method (blue, dashed lines).

which closely resembles the expected one,

$$\mathbf{B} = \begin{bmatrix} \mathbf{0} \\ \mathbf{M}^{-1} \end{bmatrix}.$$

The comparison of the computed eigenvectors is presented in Fig. 14 where again the higher error is the vector which presents the lowest error in the real and imaginary part, which is also the most damped one.

The measured excitation method seems to perform slightly worse than the one which does not directly use the information related to the input. This is probably due to the fact that the computed matrix $\mathbf{\Sigma_{xu}}$ contains larger errors than the one that can be theoretically obtained from Eq. (69). In this case the N4SID algorithm using the information gained from the input time history outperforms the method here presented.

## 5. Final remarks

The work here presented stems from the need to interpret proper orthogonal modes to understand how it is possible to recover information related to the eigensolution of the system under analysis. As a result, an approach to the identification of the eigensolutions of systems from free and forced response is presented, based on deterministic auto- and cross-covariances. The use of cross-covariances allows accurate estimates of state space representations of linear systems when they are not stationary. This allows to add the required information to the characteristic covariance matrices needed to recover the correct eigensolutions from the proper orthogonal decomposition in any condition. Identification from free responses may suffer from the presence of disturbances; this is mitigated by considering the forcing terms in the identification. When the knowledge of the input is not exploited interesting results are obtained from the simultaneous solution of a Lyapunov-like and a non-symmetric Riccati-like algebraic equation (when the input represents a good approximation of band-limited white random noise). To our knowledge the problem has not been presented in this form yet. Analytical and numerical results illustrate the soundness of the approach in simple, yet significant applications.

The ''unknown excitation'' method seems to perform always better than the one tagged as ''measured excitation'', so it should be used in any case. However, the last one gives the additional estimate of the input distribution matrix. Improvement on this side may come from better numerical representation of white noise processes or from exploiting Eqs. (62), (63), for a general non-white noise measured input. Issues related to the capability of the input to excite all the included system dynamics certainly will arise anyhow.

Some open issues remains on the correct mathematical characterization and on a possible general solution for the ''unknown excitation'' identification equation. Future investigations will include the possibility to use the defined proper dynamic decomposition, as a system reduction method for dynamic systems, looking in

more details to its properties, and the possible insight into the system under investigation when nonlinear cases are considered.

## References

[1] G. Kerschen, J.-C. Golinval, A. Vakakis, L. Bergman, The method of proper orthogonal decomposition for dynamical characterization and order reduction of mechanical systems: An overview, *Nonlinear Dynamics* 41 (1–3) (2005) 147–169.
[2] I.T. Jolliffe, *Principal Component Analysis*, second ed., Springer, New York, NY, 2002.
[3] K. Pearson, On lines and planes of closest fit to system of points in space, *Philosophical Magazine* 2 (6) (1901) 559–572.
[4] H. Hotelling, Analysis of a complex of statistical variables into principal components, Journal of Educational Psychology 24 (1933) 417–441, 498–520.
[5] S. Bellizzi, R. Sampaio, POMs analysis of randomly vibrating systems obtained from Karhunen-Loève expansion, *Journal of Sound and Vibration* 297 (2006) 774–793.
[6] Y.K. Lin, *Probabilistic Theory Of Structural Dynamics*, McGraw-Hill, New York, NY, 1967.
[7] B. Feeny, R. Kappagantu, On the physical interpretation of proper orthogonal modes in vibrations, *Journal of Sound and Vibration* 211 (4) (1998) 607–616.
[8] G. Kerschen, J. Golinval, Physical interpretation of the proper orthogonal modes using the singular value decomposition, *Journal of Sound and Vibration* 249 (5) (2002) 849–865.
[9] B. Feeny, Y. Liang, Interpreting proper orthogonal modes of randomly excited vibration systems, *Journal of Sound and Vibration* 265 (2003) 953–966.
[10] G. Quaranta, P. Masarati, P. Mantegazza, Dynamic characterization and stability of a large size multibody tiltrotor model by POD analysis, *ASME 19th Biennial Conference on Mechanical Vibration and Noise* (*VIB*), Chicago IL, 2003.
[11] G. Quaranta, P. Masarati, P. Mantegazza, Assessing the local stability of periodic motions for large multibody nonlinear systems using POD, *Journal of Sound and Vibration* 271 (3–5) (2004) 1015–1038.
[12] S. Han, B. Feeny, Application of proper orthogonal decomposition to structural vibration analysis, *Mechanical System and Signal Processing* 17 (5) (2003) 989–1001.
[13] D. Chelidze, W. Zhou, Smooth orthogonal decomposition-based vibration mode identification, *Journal of Sound and Vibration* 292 (3–5) (2006) 461–473.
[14] F. Tisseur, K. Meerbergen, The quadratic eigenvalue problem, *SIAM Review* 43 (2) (2001) 235–286.
[15] A. Preumont, *Random Vibration and Spectral Analysis of Solid Mechanics and its Applications*, Vol. 33, Kluwer Academic Publishers, Dordrecht, The Netherlands, 1994.
[16] R. Skelton, I. Iwasaki, K. Grigoriadis, *A Unified Algebraic Approach to Linear Control Design*, Taylor & Francis, London, UK, 1998.
[17] L. Ljung, *System Identification: Theory for the User*, Prentice-Hall, Inc., Upper Saddle River, NJ, USA, 1986.
[18] G.H. Golub, C.F. van Loan, *Matrix computation*, second ed., John Hopkins University Press, Baltimore, 1991.
[19] A. Bryson, Y. Ho, *Applied Optimal Control*, Wiley, New York, 1975.
[20] P. Van Overschee, B. De Moor, N4SID: subspace algorithms for the identification of combined deterministic-stochastic systems, *Automatica* 30 (1) (1994) 75–93.